AD-A112 466 CANYON RESEARCH GROUP INC WESTLAKE VILLAGE CA F/G 1/2
REPORTS BY SYSTEMS TECHNOLOGY, INC., IN SUPPORT OF CARRIER-LAND--ETC(U)
DEC 81 W F JEWELL, H R JEX, R E MAGDALENO N61339-78-C-0060
UNCLASSIFIED TR-81-025 NAVTRAEQUIPC-78-C-0060-10 NL

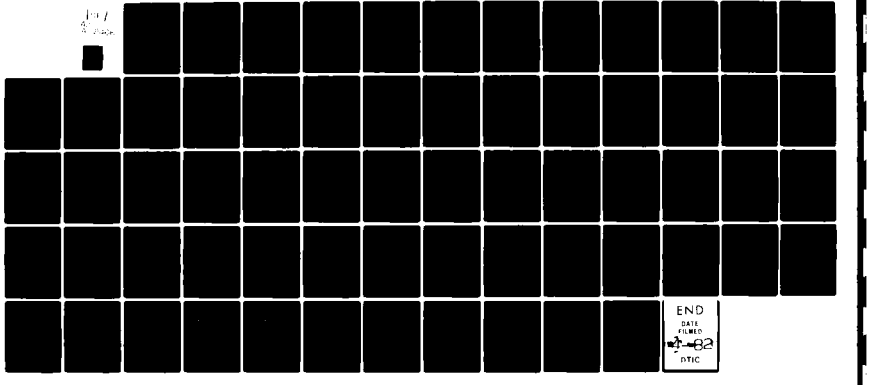

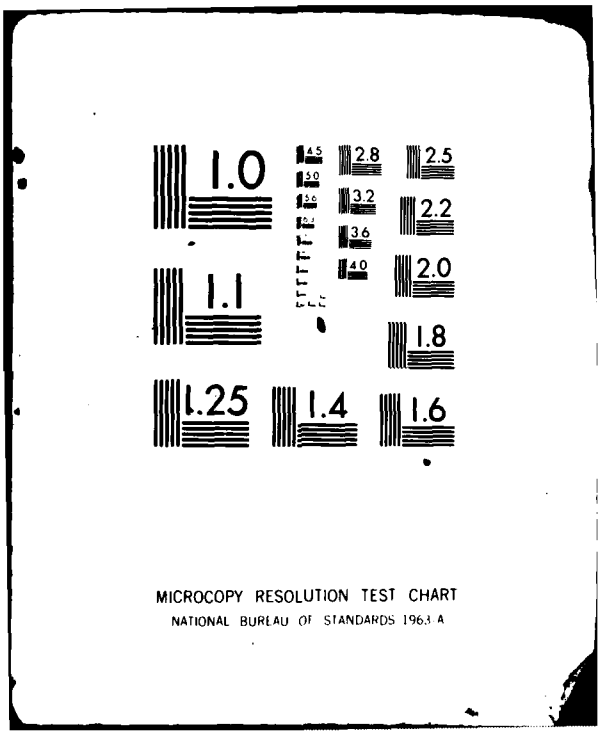
1.0
1.1
1.25
1.4
1.6
1.8
2.0
2.2
2.5
2.8
3.2
3.6
4.0
4.5
5.0
5.6
MICROCOPY RESOLUTION TEST CHART
NATIONAL BUREAU OF STANDARDS 1963 A

(1)

AD A112466

DTIC FILE COPY

DTIC
ELECTE
MAR 25 1982
S
E

Canyon Research Group, Inc.

82 03 22 138

NAVTRAEQUIPCEN 78-C-0060-10

REPORTS BY SYSTEMS TECHNOLOGY, INC., IN SUPPORT OF CARRIER-LANDING RESEARCH IN THE VISUAL TECHNOLOGY RESEARCH SIMULATOR

W. F. Jewell; H. R. Jex;
R. E. Magdaleno; and R. F. Ringland
SYSTEMS TECHNOLOGY, INC.

CANYON RESEARCH GROUP, INC.
741 Lakefield Road, Suite B
Westlake Village, California 91361

Interim Report for Period
1 May 1980 - 30 November 1981

Prepared for:

NAVAL TRAINING EQUIPMENT CENTER
Orlando, Florida 32813

Technical Report NAVTRAEQUIPCEN 78-C-0060-10

REPORTS BY SYSTEMS TECHNOLOGY, INC., IN SUPPORT OF CARRIER-LANDING RESEARCH IN THE VISUAL TECHNOLOGY RESEARCH SIMULATOR

Canyon Research Group, Inc.
741 Lakefield Road, Suite B
Westlake Village, California 91361

Interim Report for Period
1 May 1980 - 30 November 1981

Prepared for:

NAVAL TRAINING EQUIPMENT CENTER
Orlando, Florida 32813

UNCLASSIFIED

SECURITY CLASSIFICATION OF THIS PAGE (When Data Entered)

REPORT DOCUMENTATION PAGE	READ INSTRUCTIONS BEFORE COMPLETING FORM
1. REPORT NUMBER: NAVTRAEQUIPCEN 78-C-0060-10	2. GOVT ACCESSION NO.: AD-A112 206
3. RECIPIENT'S CATALOG NUMBER	
4. TITLE (and Subtitle): REPORTS BY SYSTEMS TECHNOLOGY, INC., IN SUPPORT OF CARRIER-LANDING RESEARCH IN THE VISUAL TECHNOLOGY RESEARCH SIMULATOR	5. TYPE OF REPORT & PERIOD COVERED: INTERIM 1 May 1980 - 30 November 1981
	6. PERFORMING ORG. REPORT NUMBER: TR-81-025
7. AUTHOR(s): W. F. Jewell, H. R. Jex, R. E. Magdaleno, and R. F. Ringland	8. CONTRACT OR GRANT NUMBER(s): N61339-78-C-0060
9. PERFORMING ORGANIZATION NAME AND ADDRESS: Canyon Research Group, Inc. 741 Lakefield Road, Suite B Westlake Village, California 91361	10. PROGRAM ELEMENT, PROJECT, TASK AREA & WORK UNIT NUMBERS: 4781-6P1A
11. CONTROLLING OFFICE NAME AND ADDRESS: NAVAL TRAINING EQUIPMENT CENTER Orlando, Florida 32813	12. REPORT DATE: December 1981
	13. NUMBER OF PAGES: 59
14. MONITORING AGENCY NAME & ADDRESS(if different from Controlling Office)	15. SECURITY CLASS. (of this report): UNCLASSIFIED
	15a. DECLASSIFICATION/DOWNGRADING SCHEDULE

16. DISTRIBUTION STATEMENT (of this Report)

Approved for public release; distribution unlimited.

17. DISTRIBUTION STATEMENT (of the abstract entered in Block 20, if different from Report)

18. SUPPLEMENTARY NOTES

19. KEY WORDS (Continue on reverse side if necessary and identify by block number)

Flight Simulation
Flight Models
Turbulence
Carrier Landing
Performance Measurement

20. ABSTRACT (Continue on reverse side if necessary and identify by block number)

This report contains a series of papers prepared by Systems Technology, Inc., (STI) in support of carrier-landing research in the Visual Technology Research Simulator (VTRS). The following work was undertaken:

1. Development of a quasi-random turbulence model. This model was preferred to the one provided initially with the VTRS system because it enabled better analysis of pilot responses to turbulence inputs. The

DD FORM 1 JAN 73 1473 EDITION OF 1 NOV 65 IS OBSOLETE

UNCLASSIFIED

20. ABSTRACT (Cont'd)

STI model is expected to be appropriate for tasks other than carrier landings and for simulations of other aircraft types.

2. Modification of the T-2C simulation to more closely represent the A-7 and F-18 aircraft.

3. Application and evaluation of STI's Non-Intrusive Pilot Identification Program (NIPIP), which was developed to estimate the pilot's input-output describing function and combined pilot-vehicle performance parameters such as crossover frequency and phase margin by using a time domain model of the pilot and a least-squares identification algorithm. NIPIP functions in real-time and uses a "sliding" time window to maintain freshness in the data; thus time-varying characteristics in the pilot's control strategy can be measured.

It was proposed to evaluate this technique for its application to VTRS research. STI could possibly identify pilot behavioral variations as a function of task changes on dependent measures of:

1. Pilot input bandwidth;
2. Pilot stability margin; and
3. Crossfeed control.

In particular, development of proper crossfeed control might be a good criterion of learning for glide slope control. The novice pilot is unlikely to be able to coordinate power and pitch adjustments in an optimum manner. The NIPIP program may be able to identify development of crossfeed control, or any breakdown in the strategy, and thus could provide a valuable supplement to the existing performance measurement package.

The first set of data supplied to STI to test NIPIP was unsuitable for complete analysis because of errors in the turbulence model used during data collection. More data were collected and were used to analyze selected runs from an aircraft simulation of the T-2C on final approach to an aircraft carrier. The NIPIP results presented demonstrated changes in the pilot's describing functions with simulated glide slope disturbances (injected beam noise) and the "tight" versus "loose" tracking runs. For the "loose" tracking runs, there was a very low glide slope gain and virtually no crossfeed gain. For the "tight" tracking runs, the pilot exhibited high glide slope and crossfeed gains with relatively low variability in the data, especially for the runs with beam noise. One conclusion is that the NIPIP technique can identify the pilot's control strategy and behavior by parameters meaningful to the closed-loop control task. Another implication is that adequate glide slope disturbances must be present in order for the pilot to demonstrate his ability to control the aircraft properly.

TABLE OF CONTENTS

Section		Page
I	INTRODUCTION	1
II	QUASI-RANDOM GUST INPUT FOR THE T-2C SIMULATION AT NTEC	3
	The Problem	3
	The Approach	4
	Results	5
	References	11
III	REVIEW OF THE NTEC T-2C LANDING SIMULATOR MATHEMATICAL MODEL AND ITS MODIFICATION TO A FLEET-LIKE FIGHTER	12
	Introduction	12
	Model Review	12
	Model Modification	15
	Pilot Loop Closure Topologies	19
	Summary	25
	References	26
IV	APPLICATION OF THE NON-INTRUSIVE PILOT IDENTIFICATION PROGRAM TO A MULTI-LOOP CONTROL TASK	27
	Introduction and Background	27
	Description of the Experiment	29
	Analysis	34
	Conclusions and Observations	51
	Pitch Loop	51
	Crossfeed	52
	Glide Slope	53
	Summary	53
	References	55

LIST OF TABLES

SECTION II

Table No.		Page
1	Gust Input Spectra for T-2C Landing Simulation	6

SECTION III

1	T-2C Power Approach Deviation Comparison	14
2	T-2C Transfer Function Factors for Power Approach (Corrected Derivations)	16
3	Derivative Comparison, Modified T-2C Simulation with Fleet Aircraft	18

SECTION IV

1	Gust Input Spectra for T-2C Landing Simulation	31
2	FLOLS Beam Noise	32
3	Summary of Experimental Matrix	33

LIST OF FIGURES

SECTION II

Figure No.		Page
1	Typical Airspeed Gust Waveform	7
2	Typical Crosswind Gust Waveform	8
3	Typical Vertical Gust Waveform	9

SECTION III

1	Loop Structures for Carrier Approach	21

SECTION IV

1	Block Diagram of Pilot-Aircraft System	28
2	Time History of Configuration No. 5b.0 (Student 0, Constant Range, Beam Noise Off)	35
3	Time History of Configuration No. 6a.0 (Student 0, Constant Range, Beam Noise On)	37
4	Time History of Configuration No. 9b.0 (Student 0, Variable Range, Beam Noise Off)	38
5	Time History of Configuration No. 10b.0 (Student 0, Variable Range, Beam Noise On)	39
6	Time History of Configuration No. 5b.2 (Student 2, Constant Range, Beam Noise Off)	40
7	Time History of Configuration No. 6a.2 (Student 2, Constant Range, Beam Noise On)	41
8	Time History of Configuration No. 9b.2 (Student 2, Variable Range, Beam Noise Off)	42
9	Time History of Configuration No. 10b.2 (Student 2, Variable Range, Beam Noise On)	43

LIST OF FIGURES (Concluded)

SECTION IV

Figure No.		Page
10	Time History of Pitch Loop Describing Function, $\hat{Y}_p^{\theta}(j\omega)$, No Beam Noise Configurations	44
11	Time History of Crossfeed Describing Function, $\hat{Y}_p^{x}(j\omega)$, No Beam Noise Configurations	45
12	Time History of Glide Slope Loop Describing Function, $\hat{Y}_p^{\epsilon}(j\omega)$, No Beam Noise Configurations	46
13	Time History of Pitch Loop Describing Function, $\hat{Y}_p^{\theta}(j\omega)$, With Beam Noise Configurations	47
14	Time History of Crossfeed Describing Function, $\hat{Y}_p^{x}(j\omega)$, With Beam Noise Configurations	48
15	Time History of Glide Slope Loop Describing Function, $\hat{Y}_p^{\epsilon}(j\omega)$, With Beam Noise Configurations	49

SECTION I

INTRODUCTION

This report contains a series of papers prepared by Systems Technology, Inc., (STI) in support of carrier-landing research in the Visual Technology Research Simulator (VTRS). The following work was undertaken:

1. Development of a quasi-random turbulence model. This model was preferred to the one provided initially with the VTRS system because it enabled better analysis of pilot responses to turbulence inputs. The STI model is expected to be appropriate for tasks other than carrier landings and for simulations of other aircraft types.

2. Modification of the T-2C simulation to more closely represent the A-7 and F-18 aircraft.

3. Application and evaluation of STI's Non-Intrusive Pilot Identification Program (NIPIP), which was developed to estimate the pilot's input-output describing function and combined pilot-vehicle performance parameters such as crossover frequency and phase margin by using a time domain model of the pilot and a least-squares identification algorithm. NIPIP functions in real-time and uses a "sliding" time window to maintain freshness in the data; thus time-varying characteristics in the pilot's control strategy can be measured.

It was proposed to evaluate this technique for its application to VTRS research. STI could possibly identify pilot behavioral variations as a function of task changes on dependent measures of:

1. Pilot input bandwidth
2. Pilot stability margin
3. Crossfeed control.

In particular, development of proper crossfeed control might be a good criterion of learning for glide slope control. The novice pilot is unlikely to be able to coordinate power and pitch adjustments in an optimum manner. The NIPIP program may be able to identify development of crossfeed control, or any breakdown in the strategy, and thus could provide a valuable supplement to the existing performance measurement package.

The first set of data supplied to STI to test NIPIP was unsuitable for complete analysis because of errors in the turbulence model used during data collection. More data were collected and were used to analyze selected runs from an aircraft simulation of the T-2C on final approach to an aircraft carrier. The NIPIP results presented demonstrated changes in the pilot's describing functions with simulated glide slope disturbances (injected beam noise) and the "tight" versus "loose" tracking runs. For the "loose" tracking runs, there was a very low glide slope gain and virtually no crossfeed gain. For the "tight" tracking runs, the pilot exhibited high glide slope and crossfeed gains with relatively low variability in the data, especially for the runs with beam noise. The conclusions are that a) adequate glide slope disturbances must be present in order for the pilot to demonstrate his ability to control the aircraft properly, and b) the NIPIP technique can objectively and quantitatively reveal the presence or absence and degree of a specified piloting technique during training operations.

Each of the draft reports, submitted in working-paper form by STI, is given in a separate chapter herein, along with the references for that chapter.

SECTION II

QUASI-RANDOM GUST INPUTS FOR THE T-2C SIMULATION AT NTEC

THE PROBLEM

The training scenario is simulated carrier landings in a Buckeye T-2C jet-trainer onto a carrier via the Fresnel Lens Optical Landing System (FLOLS). A number of simulator-device variables are being investigated, such as: raster-lines (1025 versus 525), brightness, motion-base (versus none), haptic seat (versus none), sea-texture (versus none), visual scene lags (approximately 0.10 sec versus 0.20 sec), pilot experience (basic-trained versus fleet-experienced), several FLOLS/carrier representations (CGI versus model/CCTV, each with fine and coarse details), and others. The carrier deck is not moving; so turbulence inputs are used to provide a relevant control task, to excite the closed-loop vehicle dynamic modes under pilot control, and to permit later analysis of selected data in more detail.

The normal simulator's "carrier-burble" is not used during this experiment. The approach takes about 55 sec, of which 40 sec are on the approach path. The pilot uses throttle to control airspeed and height, elevator to control attitude, and aileron to control lateral lineup errors, according to standard carrier landing procedures (e.g., Refs. 1 and 2*).

The gust inputs should meet the following criteria:

1. Quasi-random appearing, as perceived by the pilot, i.e., subjectively unpredictable and not easily or unavoidably learned upon subsequent encounters (to avoid learning artifacts).

---

*References for this section are given on p. 11.

2. Appreciable frequency content near the frequency regions involved in the pilot-vehicle loop closures ["phugoid," "path" (height and offset), and "short-period" and "Dutch-roll" modes).

3. Repeatable rms levels to help make the results more consistent.

4. "Realistic" and justifiable gust spectra for the turbulence behind a carrier.

5. (Desirable) — Permit later frequency domain analysis to untangle the pilot's control strategy, if needed, such as crossfeeds between elevator and throttle, effect of motion, etc.

6. Be insertable in the simulation as u_g, v_g, and w_g gusts.

THE APPROACH

A set of three independent sum-of-sinusoid inputs is ideal for the following reasons:

1. By keeping integer number of cycles over a 40 sec run length, each rms input value will be identical from run-to-run; and Fourier analyses will show distinct line spectra; while the random initial phase will provide different appearing waveforms.

2. If all frequencies are different among inputs, then crossfeeds from one axis to another may be more easily determined (by later frequency-domain analyses); and the inputs are statistically independent.

3. The frequencies may be placed to excite the very low frequency closed-loop modes more consistently and efficiently than a purely random signal.

4. The amplitudes may be shaped to match the effective power-spectral density of actual turbulence in the desired frequency range.

A check of the T-2C dynamics, based on data given in Ref. 3 and elsewhere, showed that the phugoid and path modes lie in the region from ω = 0.16 to 0.30 rad/sec (0.03 to 0.06 Hz), while the lateral roll-spiral modes lie near 0.5 to 1.0 rad/sec, the pitch short period near 2.1 rad/sec, and Dutch-roll mode near 2 to 3 rad/sec (depending on yaw damper activation). Therefore inputs spanning 0.03 to 3.0 rad/sec are desired; distributed in each axis as appropriate for its closed-loop frequency region. This requires a minimum run length of 40 sec for which the fundamental frequency is 0.025 Hz or 0.157 rad/sec.

RESULTS

After careful consideration of non-simple harmonic ratios in each axis (with the exception of the 1:3 radio in u_g, which cannot be helped), integer number of cycles in 40 sec, good dispersion on the log-frequency (Bode) plots, not-too-close spacing thereon, and no more than 4 to 5 sinusoids per axis for good signal/noise considerations; the frequencies shown in Table 1 were selected.

The gust spectral shapes were based on the actual carrier turbulence data given in Ref. 2, Appendix B.

For this special case, which is similar to but not quite the same as low altitude atmospheric turbulence, the spectral density shape in the vicinity of the gust input region was closely approximated as first-order filtered noise. To compensate for the non-uniform spacing of sinusoids, each sinusoid is assumed to cover an effective bandwidth set by the geometric mean between adjacent frequencies, and an equal spacing beyond each last one. Given the input frequencies, phases, and desired spectral envelope, a proprietary computer program computes the required amplitudes, amplitude-probability distribution, and typical waveform. Samples are included here as Figs. 1, 2, and 3.

TABLE 1. GUST INPUT SPECTRA FOR T-2C LANDING SIMULATION

Number of Cycles in 40 sec Run	Frequency		Gust Shaped Amplitudes for RMS = 1 unit in each Axis			Comments
N	f_i (Hz)	ω_i (rad/sec)	Axial (ft/sec)	Lateral (ft/sec)	Vertical (ft/sec)	Modes Excited:
1	0.025	0.157	$A_{u_1} = 0.645$			Speed and height modes ω_h''
2	0.050	0.314			$A_{w_1} = 1.175$	
3	0.075	0.471	$A_{u_2} = 0.749$			Lateral Path Modes ω_ψ''
4	0.100	0.628		$A_{v_1} = 1.295$		
5	0.125	0.785			$A_{w_2} = 0.580$	
7	0.175	1.10	$A_{u_3} = 0.707$			$1/T_{\theta_2}$
8	0.200	1.26			$A_{w_3} = 0.381$	
9	0.225	1.41		$A_{v_2} = 0.431$		
11	0.275	1.73	$A_{u_4} = 0.548$			Short Period Mode ω_{sp}
13	0.325	2.04			$A_{w_4} = 0.294$	
14	0.350	2.20		$A_{v_3} = 0.288$		
17	0.425	2.67	$A_{u_5} = 0.473$			Dutch Roll Mode ω_{DR}
19	0.475	2.83			$A_{w_5} = 0.226$	
23	0.575	3.61		$A_{v_4} = 0.234$		

$$RMS = \Sigma A_i^2/2$$

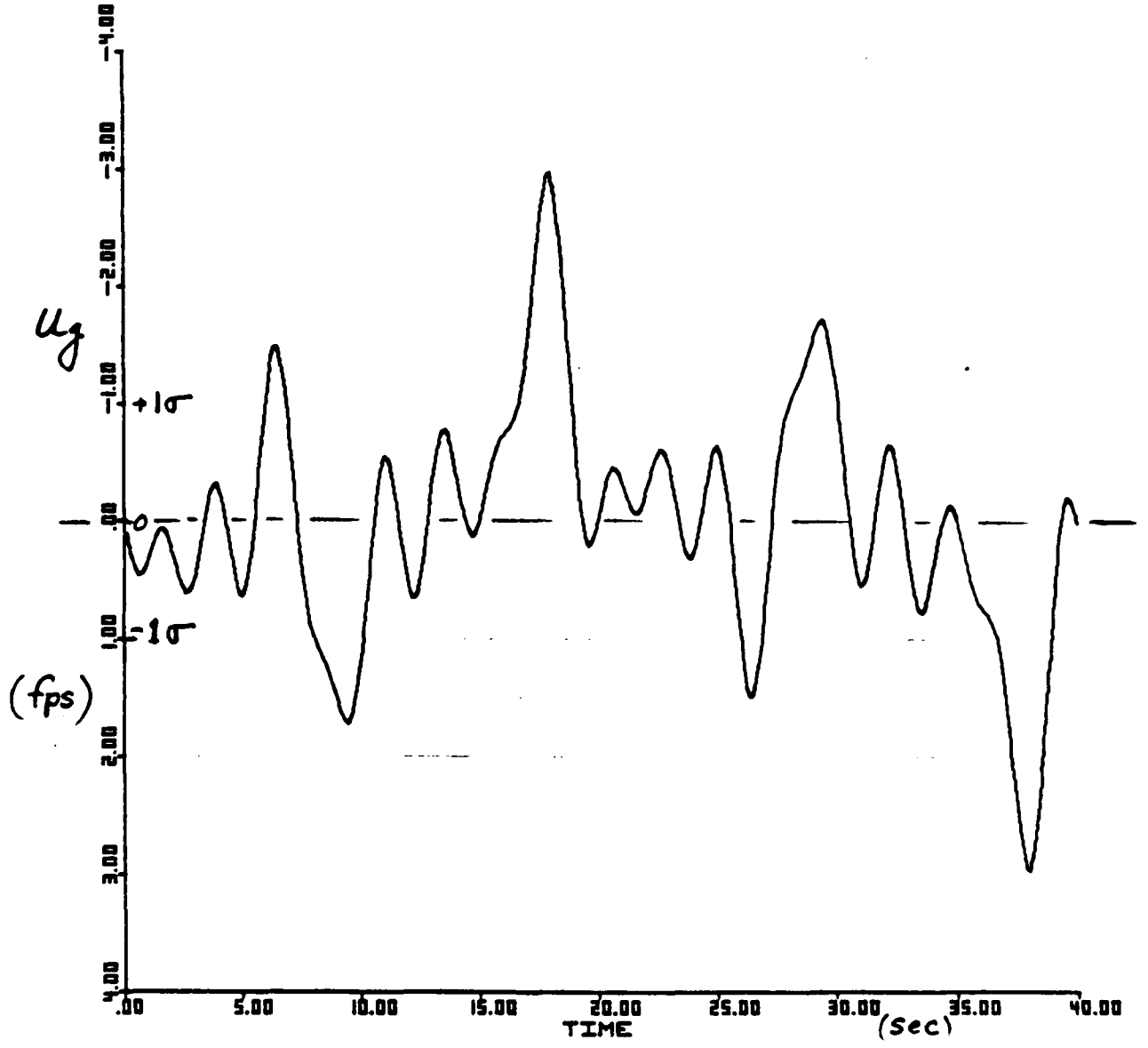

Figure 1. Typical Airspeed Gust Waveform for σ_{u_g} = 1 fps

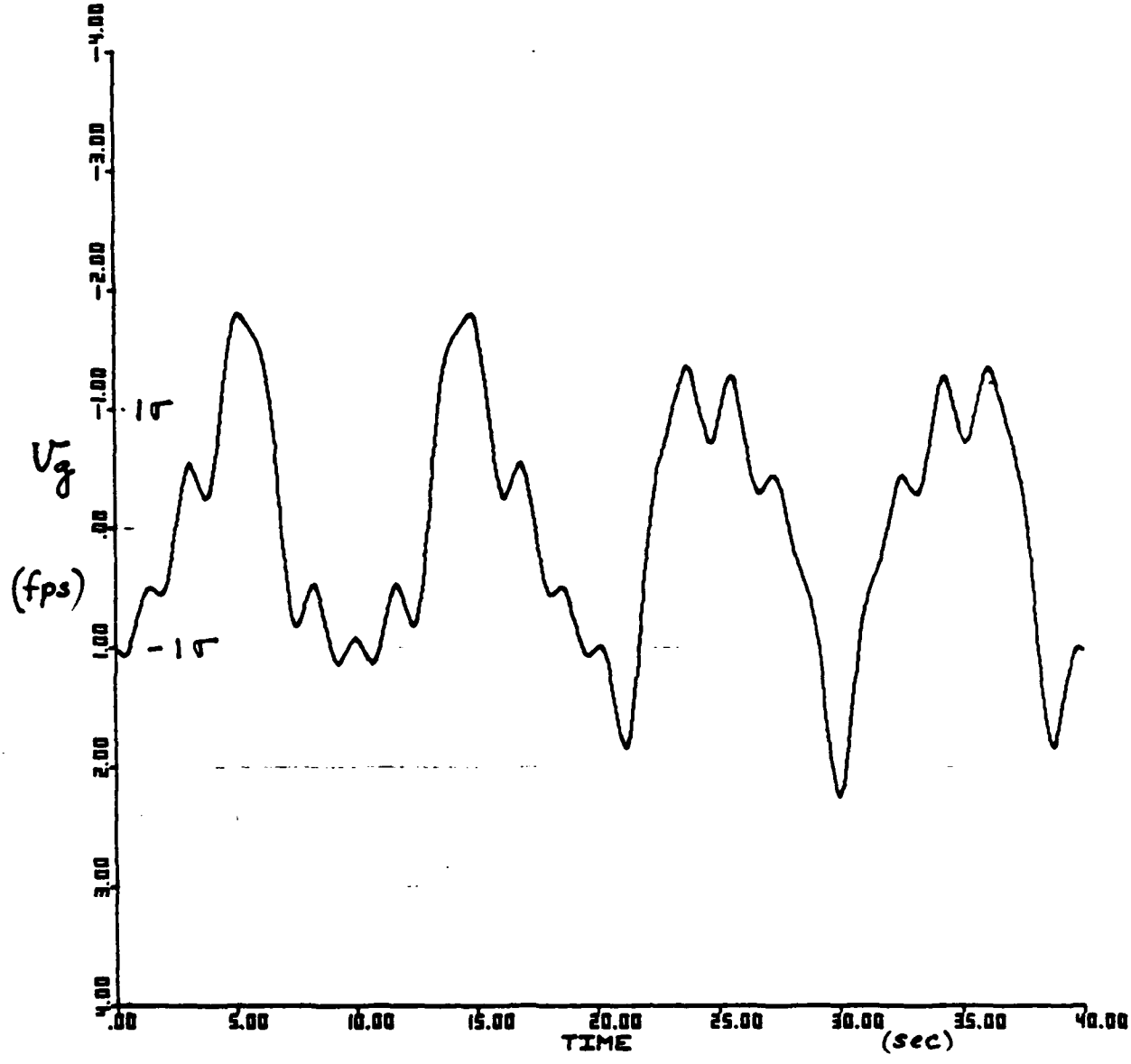

Figure 2. Typical Crosswind Gust Waveform for σ_{vg} = 1 fps

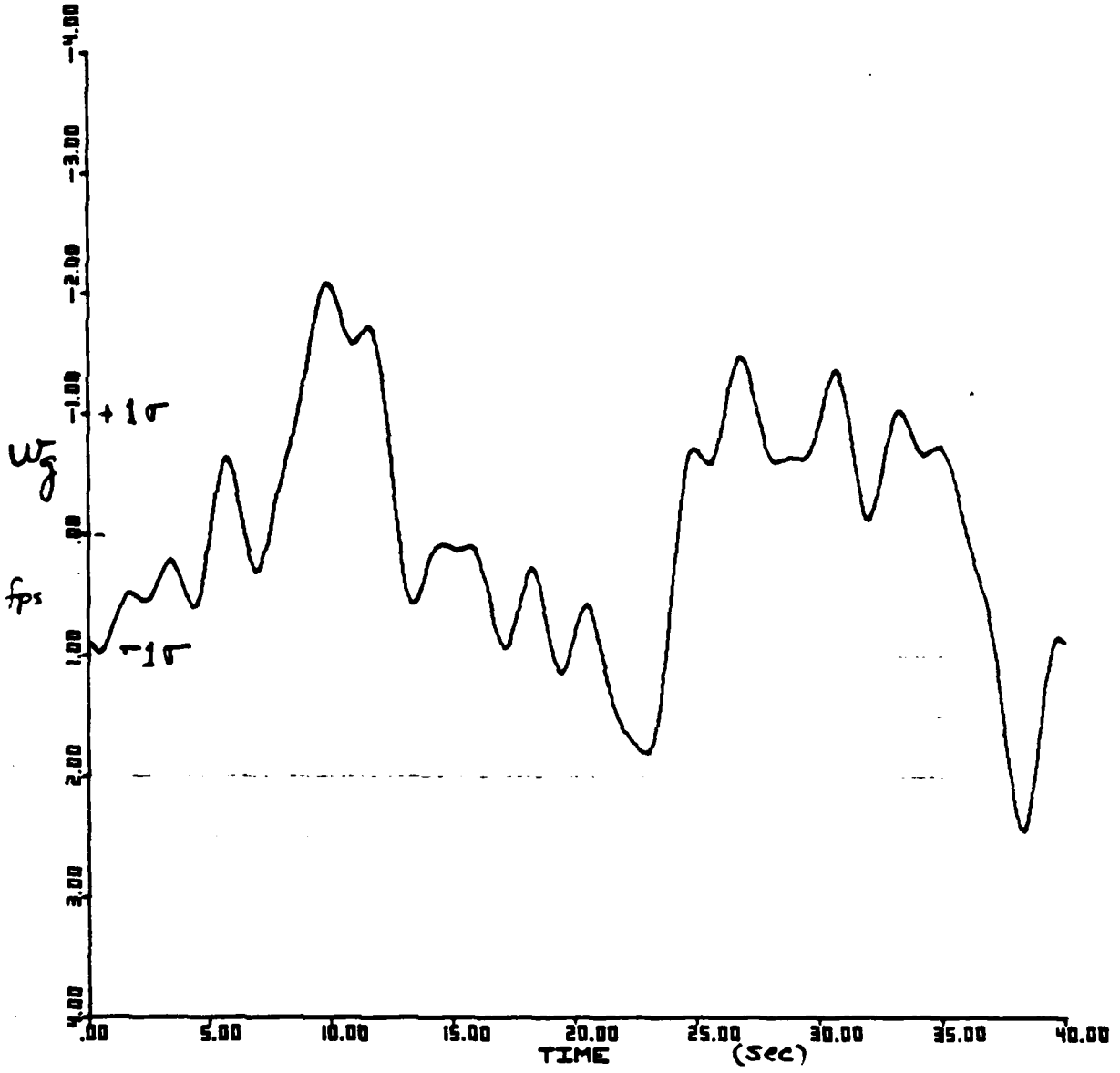

Figure 3. Typical Vertical Gust Waveform for σ_{wg} = 1 fps

Each signal spectra has been adjusted for 1 unit (e.g., ft/sec) rms value, and the sum should be multiplied by the desired turbulence intensity levels. For this carrier landing case, use the same rms gust intensity in each axis, as follows:

Gustiness	RMS Level ft/sec
Low	1.0
Moderate	3.0
Rough	5.0

We recommend 3.0 ft/sec as a representative level. Note that peak gust velocities will occasionally reach 3 to 10 ft/sec. This will not stall the wing or tails, yet is big enough to provide adequate path and motion system excitation.

Rather than provide purely randomized mutual phasing, we recommend using 3 or 4 sets (of phases), so that corresponding time traces may be overlaid for comparisons. Each of the sets should be checked for a subjectively "random" appearance, i.e., no large waveform "signatures" (which are detectable upon third encounter). They can be used in random or systematic order to avoid learning artifacts.

Even though the range to the FLOLS is varying during the approach, experience has shown that fairly stationary statistics exist along the approach path until the last 5 to 10 sec. Therefore the approach performance rms statistics should be based on the time period from 50 to 10 sec before nominal touchdown, and separate (transient-type) statistics should be used for the last 10 sec (as well as for the first 5 sec after the start of final approach).

REFERENCES FOR SECTION II

1. Durand, T. S., and R. J. Wasciko, "Factors Influencing Glide Path Control in Carrier Landings," Journal of Aircraft, Vol. 4, No. 2, March-April 1967.

2. Durand, T. S., Carrier Landing Analyses -- Final Report, Systems Technology, Inc., Technical Report No. 137-2, February 1967.

3. Buenz, D. A., et al., Identification of T-2 Aerodynamic Derivatives from Flight Data, Systems Control Inc., for Naval Air Development Center, March 1975 (AD-A021 996).

SECTION III

REVIEW OF THE NTEC T-2C LANDING SIMULATOR MATHEMATICAL MODEL AND ITS MODIFICATION TO A FLEET-LIKE FIGHTER

INTRODUCTION

Simulator tests of a modified FLOLS visual landing aid (the rate-error display bars of Lt. C. Kaul) are currently being planned for the simulator at the Naval Training Equipment Center in Orlando, Florida. The aircraft mathematical model was reviewed with a view to modifying its characteristics to resemble current Navy fighters, thereby providing a carrier approach task more representative of fleet operations which might benefit from the improved FLOLS display. The major data source is an NTEC FORTRAN listing of the "Aerodynamic Subroutine" which models the T-2C, supplemented by an antecedent document, the Singer Link T-2C simulation subroutines (Ref. 1*).

MODEL REVIEW

The NTEC FORTRAN listing, dated 17 July 1980, was reviewed and compared against the Sinker Link routines in Ref. 1; and the resulting "non-dimensional" aerodynamic force and moment equations were abstracted in the format of Ref. 2. The following anomalies were noted:

1. The sign of Z_{δ_e} (due to $C_{L_{\delta_e}}$) appears incorrect. For aft horizontal tail, deflection of the elevator (e.g., T_E up) should result in the tail's pitching moment

*References for Section III are on p. 26.

(positive nose up) and the z-axis force (positive downward) being of the same sign.

2. The sign of $C_{M_{\dot{\alpha}}}$ appears incorrect. For subsonic aircraft, the sign of this term should be the same as C_{M_q}. Also, a modification has been inserted in the code multiplying this coefficient by 0.47.

3. The combination of $[C_{M_q}q + 0.47C_{M_{\dot{\alpha}}}\dot{\alpha}]$ is multiplied by a factor of 4.0, resulting in a computed value for M_q approximately 4 times that given for the T-2C in Table 11 of Ref. 3 for a similar flight condition.

It is hypothesized that these errors tend to cancel each other from the viewpoint of the pilot in the cab. Certainly increased aircraft damping would tend to mitigate the otherwise abrupt normal acceleration response to elevator deflection. It would also tend to negate the destabilizing tendency associated with the positive sign on $C_{M_{\dot{\alpha}}}$.

The errors were corrected and dimensional coefficients were calculated for comparison with the data of Ref. 3 and the wind tunnel data cited in Ref. 4. This comparison is shown in Table 1. Experience relating various derivatives to response dynamics (e.g., Ref. 2) suggests substantial agreement for the derivatives affecting high- and mid-frequency responses. Some differences are apparent in the derivatives affecting low-frequency speed-related responses, which may be attributable to differences in flaps, speed brake, or landing gear positions.

TABLE 1. T-2C POWER APPROACH DEVIATION COMPARISON

Parameter	Units	"Corrected" Simulation	Ref. 3	Ref. 4
Velocity	(kt) ft/sec	(108) 183	(108) 183	(139.6) 236
Weight	lb	11,000	11,000	1,000
α_{trim}	deg	6.99	4.0*	4.7
Flap	deg	33.	--	16.
Speed brake	deg	0	--	.0
Gear		Down	--	Down
X_u	sec^{-1}	- 0.0742	- 0.046	- 0.046
Z_u	sec^{-1}	- 0.3427	- 0.2206	- 0.269
M_u	$(ft\text{-}sec)^{-1}$	0.00092	--	0.00434
$M_{\dot{w}}$	ft^{-1}	- 0.002249	- 0.002	- 0.00225
X_w	sec^{-1}	- 0.1350	0.0534	- 0.0983
Z_w	sec^{-1}	- 0.7384	- 0.7683	- 0.974
M_w	$(ft\text{-}sec)^{-1}$	- 0.01531	- 0.0168	- 0.01945
M_q	sec^{-1}	- 1.1593	- 1.105	- 1.42
X_{δ_e}	ft/sec^2	- 6.987	--	--
Z_{δ_e}	ft/sec^2	-15.54	014.45	-24.07
M_{δ_e}	sec^{-2}	- 5.187	- 5.824	- 9.63
X_{δ_T}	$ft/lb\text{-}sec^2$	0.002904	--	--
Z_{δ_T}	$ft/lb\text{-}sec^2$	- 0.000352	--	--
M_{δ_T}	$(lb\text{-}sec^2)^{-1}$	0.0000363	--	--

*Based on stated value of thrust line inclination relative to stability axes of +0.07 rad (+4.0 deg).

Table 2 lists some of the more important transfer function parameters associated with the corrected simulation data*. Comparison with handling qualities experience (e.g., Ref. 2) shows the airplane to be "well behaved" in its attitude responses (well-damped short period near 2 rad/sec), slightly on the backside (small negative value for $1/T_{d_1}$), with adequate path angle response bandwidth ($1/T_{\theta_2} > 0.7$). Because the throttle response lag for the T-2C is relatively short, on the order of 0.25 sec, the path response to the throttle is good, as is the path response to attitude change. The aircraft also exhibits a modest pitch up with power application.

Either the conventional CTOL (primary emphasis on attitude change for path correction) or the "Navy doctrinal" (primary emphasis on throttle for path correction) techniques are usable for this airplane, the former with some modification to correct for "backsidedness" —— being on the "back side" of the power-required curve (i.e., below minimum-power speed).

MODEL MODIFICATIONS

To make the T-2C behave more like a typical Navy fighter on carrier approach or, more particularly, to make it behave like an aircraft known to have less than desirable handling qualities for this task requires that the path responses to throttle and elevator be determined. The A-7 (Ref. 5) and F-18-like (Ref. 6) aircraft provide good examples. The changes (relative to the "corrected simulation" of the T-2C) required to deteriorate the responses are as follows:

---

*A common shorthand format is used to list the first- and second-order dynamics:

high-frequency gain $\equiv$ xxx; $(s + 1/T) \equiv (1/T)$; $[s^2 + 2\zeta\omega s + \omega^2] \equiv [\zeta, \omega]$

TABLE 2. T-2C TRANSFER FUNCTION FACTORS FOR POWER APPROACH (CORRECTED DERIVATIVES)

Format is: Gain (1/T) $[\zeta_n, \omega_n]$

Denominator

$$\Delta = [0.0653,\ 0.200]_{\zeta_{sp}\ \omega_{sp}}\ [0.614,\ 1.919]_{\zeta_{sp}\ \omega_{sp}}$$

Elevator Numerators

$$N^{\theta}_{\delta_e} = -5.15_{1/T_{\theta_1}}(0.01552)_{1/T_{\theta_2}}(0.756)$$

$$N^{\dot{d}}_{\delta_e} = 15.54_{1/T_{d_1}}(-0.0695)_{1/T_{d_2}}(-5.77)_{1/T_{d_3}}(7.33)$$

$$N^{u}_{\delta_e} = -6.99_{1/T_{u_1}}(0.420)_{1/T_{u_2}}(-5.54)_{1/T_{u_3}}(7.13)$$

Throttle Numerators

$$N^{\dot{d}}_{\delta_T} = 0.000352(0.303)[0.466,\ 4.48]$$

$$N^{u}_{\delta_T} = 0.00290(-0.1106)[0.678,\ 1.796]$$

Coupling Numerators (Throttle and Elevator

$$N^{u\ \theta}_{\delta_T \delta_e} = -0.01470(0.716)$$

$$N^{\dot{d}\ \theta}_{\delta_T \delta_e} = -0.00239(2.18)$$

1. Airspeed of 130 kt (219 ft/sec) — like the A-7.

2. Flaps to 16 deg, speed brakes fully extended, gear down.

3. Lift equation changes (provides required C_L and $\partial C_L/\partial\alpha$ at the desired value of α):

   AFKCLALP = 0.65
   AFKCLFLP = 1.38
   AFKCLWKR = 0

4. Drag equation changes (provides required C_D and $\partial C_D/\partial\alpha$):

   AFKCDCL = 1.51
   AFKCDSB = 1.18
   AFKCDFW = 0

5. Engine equivalent time constant, T_E = 1.0 sec.

Table 3 lists the resulting stability derivatives and compares them with the A-7 and F-18-like data of Refs. 5 and 6. Appended to the table is a selected set of transfer function factors. These data suggest that the path responses would be similar for the three cases. The short-period response differences are not so great as indicated because both the A-7 and F-18-like aircraft are modified by their flight control systems to revise their effective short-period frequencies.

With regard to its path responses to either the stick (attitude change) or the throttle, the modified T-2C should exhibit properties similar to those of the A-7 and F-18. In brief, the pilot will find it difficult to fly on approach because its responses simply are not fast enough [slow engine, long (2+ sec) path response lag, T_{θ_2}]. Further, the closure rate is similar to that of the other two aircraft, which should present the pilot with similar time-to-go stress and perceptual-range difficulties (Ref. 7).

All three aircraft suffer from deficient responses in the "outer" control loop for precision path control in carrier approach — deficient in the sense that they are not fast enough and (possibly barring the F-18

TABLE 3. DERIVATIVE COMPARISON, MODIFIED T-2C SIMULATION WITH FLEET AIRCRAFT

Parameter	Units	Modified T-2C Simulation	A-7 (Ref. 5)	F-18-Like (Ref. 6)
Velocity	ft/sec	219	218	226
Weight	lb	13,200	24,000	27,890
α_{trim}	deg	6.9	12.0	5.5
X_u	sec^{-1}	- 0.0608	- 0.0545	- 0.0691
Z_w	sec^{-1}	- 0.2865	- 0.2870	- 0.2950
M_u	$(ft\text{-}sec)^{-1}$	- 0.000755	- 0.000165	0
$M_{\dot{w}}$	ft^{-1}	- 0.002249	- 0.000289	- 0.0003167
X_w	sec^{-1}	0.0674	0.0643	0.0777
Z_w	sec^{-1}	- 0.6008	- 0.5289	- 0.4822
M_w	$(ft\text{-}sec)^{-1}$	- 0.01221	- 0.007964	- 0.001677
M_q	sec^{-1}	- 1.387	- 0.3275	- 0.2333
X_{δ_e}	$(ft\text{-}sec)^2$	- 3.379	0.7328	4.549
Z_{δ_e}	ft/sec^2	-22.16	-14.71	-17.43
M_{δ_e}	sec^{-2}	- 7.141	- 2.189	- 1.75
X_{δ_T}	$ft/lb\text{-}sec^2$	0.002903	0.001317	0.00148
Z_{δ_T}	$ft/lb\text{-}sec^2$	0.000353	- 0.000250	- 0.0001106
M_{δ_T}	$(lb\text{-}sec^2)^{-1}$	0.000036	0.000004	0.
ω_{sp}	rad/sec	1.88	1.38	0.71
ζ_{sp}				
$1/T_{\theta_2}$	1/sec	0.522	0.429	0.397
$1/T_{d_1}$	1/sec	0.0232	0.0030	0.0246
T_E	sec	1.0	1.0	0.54

with its faster engine) that they force the pilot to make path corrections with the elevator when throttle response delay becomes critical.

All three aircraft will benefit if low-frequency path deviation rate ("lead equalization") is introduced in the outer loop. The modified FLOLS scheme offers this potential by providing the pilot with an explicit indication of path error rate. We would expect to see improved pilot opinion (due to workload reduction) and perhaps even improved performance with such a scheme. The improvement should be more noticeable with more difficult aircraft.

PILOT LOOP CLOSURE TOPOLOGIES

Among the measurements which have been proposed for this experiment is the determination of pilot describing functions in the longitudinal anproach task. These will endeavor to establish pilot gain and equalization in the several loops, hence the control technique being employed. The material which follows describes the loop closure possibilities.

Common to all is control of pitch attitude with elevator, the perceptual cue coming from the pilot's awareness of where the aircraft nose is relative to the horizon, or, failing this (e.g., at night), from the carrier lights themselves. If this loop is closed loosely, subsequent closures of path deviation to either throttle or attitude are limited to low frequencies in the vicinity of the phugoid mode. If, on the other hand, the attitude loop is closed tightly, it becomes possible to achieve higher path-control response bandwidths, limited by $1/T_{\theta_2} \doteq -Z_w$. This can be accomplished with outer-loop path deviation closures to either the attitude command or to the throttle, provided that the pilot's control technique corrects for the airspeed deviations otherwise incurred. Since he does not have a head-up indication of speed (both his angle-of-attack indexer and the perceived closure rate to the carrier are poor indicators of airspeed), the skilled pilot generally accomplishes this via "cross-feeds" to the other control.

Consider first the preferred ("Navy doctrine") technique —— path control via the throttle with a tight attitude closure via elevator. Figure 1a shows the topology of the control loop structure with the addition of a crossfeed from the throttle to the attitude command. With a tight attitude loop closure the phugoid mode is driven into the attitude numerator zeros, the short-period mode to higher frequencies such that the path deviation response to thrust changes can be approximated by (thrust lag ignored):

$$\left.\frac{d}{\delta_T}\right|_{\theta \to \delta_e} \doteq \frac{N^{d\,\theta}_{\delta_T \delta_e}}{(s) N^{\theta}_{\delta_e}[\zeta'_{sp}, \omega'_{sp}]}$$

which, for the T-2C, is:

$$\left.\frac{d}{\delta_T}\right|_{\theta \to \delta} = \frac{-0.00239(2.18)}{-5.15(0)(0.01552)(0.756)[\zeta'_{sp}, \omega'_{sp}]}$$

$1/T_{\theta_1}$ $1/T_{\theta_2}$ Closed-pitch loop dynamics

Clearly it turns out (Ref. 5) that the ability of the pilot to control path is limited by the lag at $1/T_{\theta_1}$ or, more precisely, by the closed-loop root resulting from $\theta \to \delta_e$.

Now suppose that the pilot is skilled enough to pull the stick so as to raise the nose slightly upon power application (this tends to occur

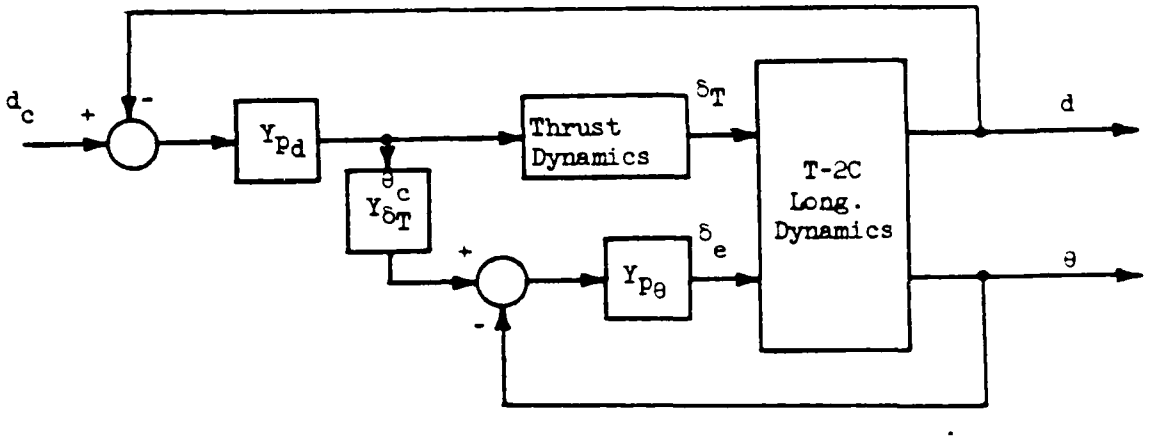

a. Navy Technique, Crossfeed for Speed Control

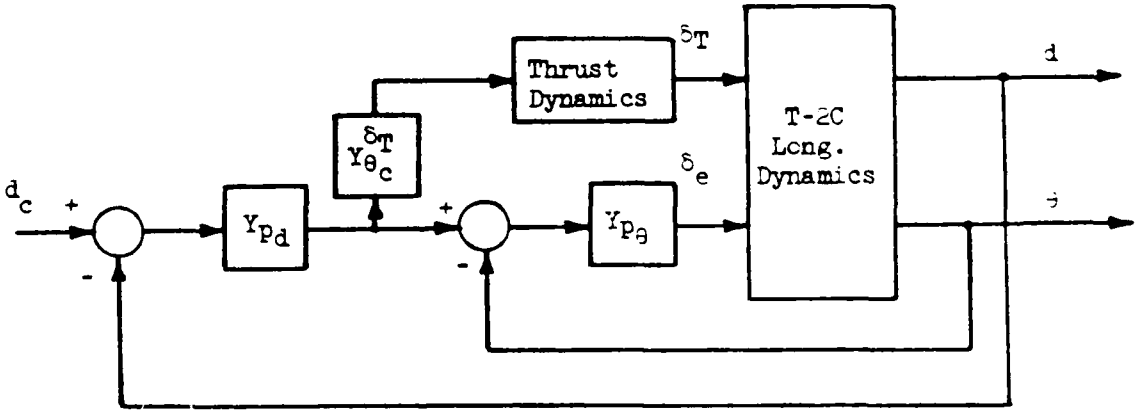

b. Conventional Technique, Crossfeed for Speed Technique

Figure 1. Loop Structures for Carrier Approach

naturally for the T-2C with its pitch-with-power characteristic) such as to minimize the resulting speed perturbation. That is:

$$\left.\frac{u}{\delta_T}\right|_{\theta \to \delta_e} = \frac{N^u_{\delta_T} \delta^{\theta}_{e}}{N^{\theta}_{\delta_e}} + Y^{\theta_e}_{\delta_e} \frac{N^u_{\delta_e}}{N^{\theta}_{\delta_e}} \doteq 0$$

This requires a crossfeed of:

$$N^{\theta_c}_{\delta_T} = -\frac{N^u_{\delta_T} \delta^{\theta}_{e}}{N^u_{\delta_e}}$$

$$\doteq \frac{-0.01470(0.716)}{-6.99(0.420)(-5.54)(7.13)}$$

which, at frequencies below 0.42 rad/sec, is equivalent to a gain $Y^{\theta_c}_{\delta_T} = 0.00009076$ rad (θ_c)/lb (δ_T). The resulting path response is given by:

$$\left.\frac{d}{\delta_T}\right|_{\substack{\theta \to \delta_e \\ \delta_T \to \theta_c}} \doteq \frac{\dot{N}^d_{\delta_T \delta_e}}{(s)N_{\delta_e}[\zeta'_{sp}, \omega'_{sp}]} + Y^{\theta_c}_{\delta_T} \frac{\dot{N}^d_{\delta_e}}{(s)N^{\theta}_{\delta_e}[\zeta'_{sp}, \omega'_{sp}]}$$

The effective numerator is:

$$\dot{N}^{d\ \theta}_{\delta_T \delta_e} + Y^{\theta_c}_{\delta_T} \dot{N}^{d}_{\delta_e} = -0.00239(2.18) + Y^{\theta_c}_{\delta_T} 15.54(-0.0695)(-5.77)(7.33)$$

which can be approximated at low frequencies by:

$$N^{\dot{d}}_{\delta_T} N^{\theta}_{\delta_e} + Y^{\theta_c}_{\delta_T} N^{\dot{d}}_{\delta_e} \doteq -0.06204(0.01716)$$

The resulting response is:

$$\left.\frac{d}{\delta_T}\right|_{\substack{\theta \to \delta_e \\ \delta_T \to \theta}} = \frac{-0.06204(0.01716)}{-5.15(0)(0.01552)(0.756)[\zeta'_{sp}, \omega'_{sp}]}$$

Approximately cancels $1/T_{\theta_1}$

$1/T_{\theta_1}$ $1/T_{\theta_2}$

Now the dominant performance-limiting lag is at $1/T_{\theta_2}$, considerably higher than before.

Some remarks and caveats:

1. Cutting the crossfeed gain to about 60 percent of the value given here shifts the zero to the vicinity of 0.07, which represents a more realistic value of $1/T'_{\theta_1}$, the closed-loop speed response dynamics.

2. Thrust response lag will limit the bandwidth of the $d \to \delta_T$ closure. Here it has been improved because $T_E = 0.25$ sec for the T-2C, considerably faster than the 2 sec (or thereabouts) closed-loop path response lag obtainable with this technique.

3. While speed perturbations are minimized, it will still be necessary to close a $u \to \delta_T$ loop intermittently to counter the effects of the carrier wake "burble." Actually, skilled pilots may even act, to a degree, "precognitively" on this; i.e., knowing the carrier and wind over deck speed and direction and then range, they

put in anticipatory throttle and elevator control pulses to compensate for the burble as they pass through it.

Attention is now directed to the more conventional CTOL technique represented by the loop structure of Fig. 1b. Here again a crossfeed is introduced, this time to the throttle. It has the same purpose and, in fact, is given by the inverse of the $Y_{\delta_T}^{\theta_c}$ of the previous example. The crossfeed moves $1/T_{d_1}$, the low-frequency (right half plane in this case) zero of the $N_{\delta_T}^{d}$ numerator to the left until it "cancels" $1/T\acute{\theta}_1$, thereby allowing $d \rightarrow \theta_c$ closures of bandwidths approaching $1/T\acute{\theta}_2$, limited in this case by the short-period response dynamics of the aircraft.

In examining Fig. 1 in the context of the forthcoming experiment we note the following:

1. Describing function measurements of pilot behavior will reveal the existence of path deviation error-correlated signals on both throttle and elevator if the speed response cancelling crossfeed is in operation with either loop structure. Only if the crossfeed is absent can such measurements distinguish between the two techniques for path control.

2. Flight records, e.g., Fig. 7 of Ref. 5, suggest time-varying pilot behavior characterized by increasing pilot gains as the carrier ramp is approached. Thus it is quite likely that simpler loop structures, having less performance potential, are used early in the approach to minimize workload, while the higher-performance loop structures and gain are used later when needed. The time-varying describing functions are anticipated to show time-varying behavior as the ramp is approached.

3. The availability of outer-loop lead compensation from the modified FLOLS should ease the pilot's task with either loop topology, particularly when the path response is limited by one or more of:

   a. Low $1/T_{\theta_2}$

   b. Slow-responding engine

Thus we would anticipate that the "modified T-2C" of Table 3 might show greater improvement from rate bars in pilot opinion, and perhaps even performance, than the T-2C, per se.

4. Speed deviations caused by external gusts and turbulence are anticipated to be mostly correlated, if at all, with the throttle and stick during the final seconds of the approach. The pilot cannot perceive such errors directly; rather, he can only respond to the resulting path errors and to the changing time indication provided by his indexer. A disturbance artificially introduced on the indexer alone could reveal closed-loop usage of this indicator.

SUMMARY

This analysis has pointed out:

1. Some minor discrepancies in the T-2C simulator mathematical model which should be resolved before this simulation.

2. Simulator modifications which will result in path responses (not short-period responses) more typical of operational Navy fighters.

3. Anticipated signal correlations and trends in pilot describing function measurements.

REFERENCES FOR SECTION III

1. Anon., Visual Technology Flight Simulator (VTFS) Math Model Report, Singer-Link Division, NAVTRAEQUIPCEN75-C-0009-11, March 1977.

2. McRuer, Duane, Irving Ashkenas, and Dunstan Graham, Aircraft Dynamics and Automatic Control, Princeton University Press, 1973.

3. Smith, R. M., and N. D. Geddes, Handling Quality Requirements for Advanced Aircraft Design: Longitudinal Mode, AFFDL-TR-78-154, August 1979.

4. Buenz, D. A., et al., Identification of T-2 Aerodynamic Derivatives from Flight Data, NADC Report, March 1975 (AD-A021116).

5. Craig, S. J., R. F. Ringland, and I. L. Ashkenas, An Analysis of Navy Approach Power Compensator Problems and Requirements, Systems Technology, Inc., Technical Report No. 197-1, March 1971.

6. Ringland, R. F., and D. E. Johnston, Analytical Assessment of the F-18A Flying Qualities During Carrier Approach, Systems Technology, Inc., Technical Report No. 1090-1, Sept. 1977.

7. Clement, W. F., and R. K. Heffley, An Example of a Concept for Establishing Flight Training Media Requirements, Systems Technology, Inc., Technical Report No. 2108-1, May 1980.

SECTION IV

APPLICATION OF THE NON-INTRUSIVE PILOT IDENTIFICATION PROGRAM TO A MULTI-LOOP CONTROL TASK

INTRODUCTION AND BACKGROUND

The Navy carrier approach control task is analyzed using the Non-Intrusive Pilot Identification Program (NIPIP, Refs. 1, 2, and 3*). The result is the identification of the basic pilot control strategy in conventional feedback control terms.

The final approach to an aircraft carrier using the Fresnel Lens Optical Landing System (FLOLS) is analyzed in terms of two loops: flight path (FLOLS) control and speed (angle of attack) control. The nominal control strategy used by the pilot is depicted in the block diagram of Fig. 1. The objective of the pilot is to regulate FLOLS glide slope deviation, ϵ, and angle of attack, α, against external disturbances due to both axial gusts, u_g, and vertical gusts, w_g. The ϵ and α loops are commonly referred to as "outer loops." The pilot must also regulate pitch attitude with the elevator, which is an "inner loop."

The prescribed Navy piloting technique for controlling the aircraft is to regulate ϵ with the throttle, δ_T, and α with the elevator, δ_e (via changes in attitude, θ) — a so-called "backside" piloting technique. In reality, however, a pilot learns that he must also "crossfeed" the throttle to pitch attitude in order to achieve adequate response. That is, when the pilot makes a correction to ϵ using δ_T he also adjusts θ_x, as shown in Fig. 1. With practice a pilot will learn how much crossfeed to use for a given aircraft and approach flight condition.

---

*References for Section IV are on p. 55.

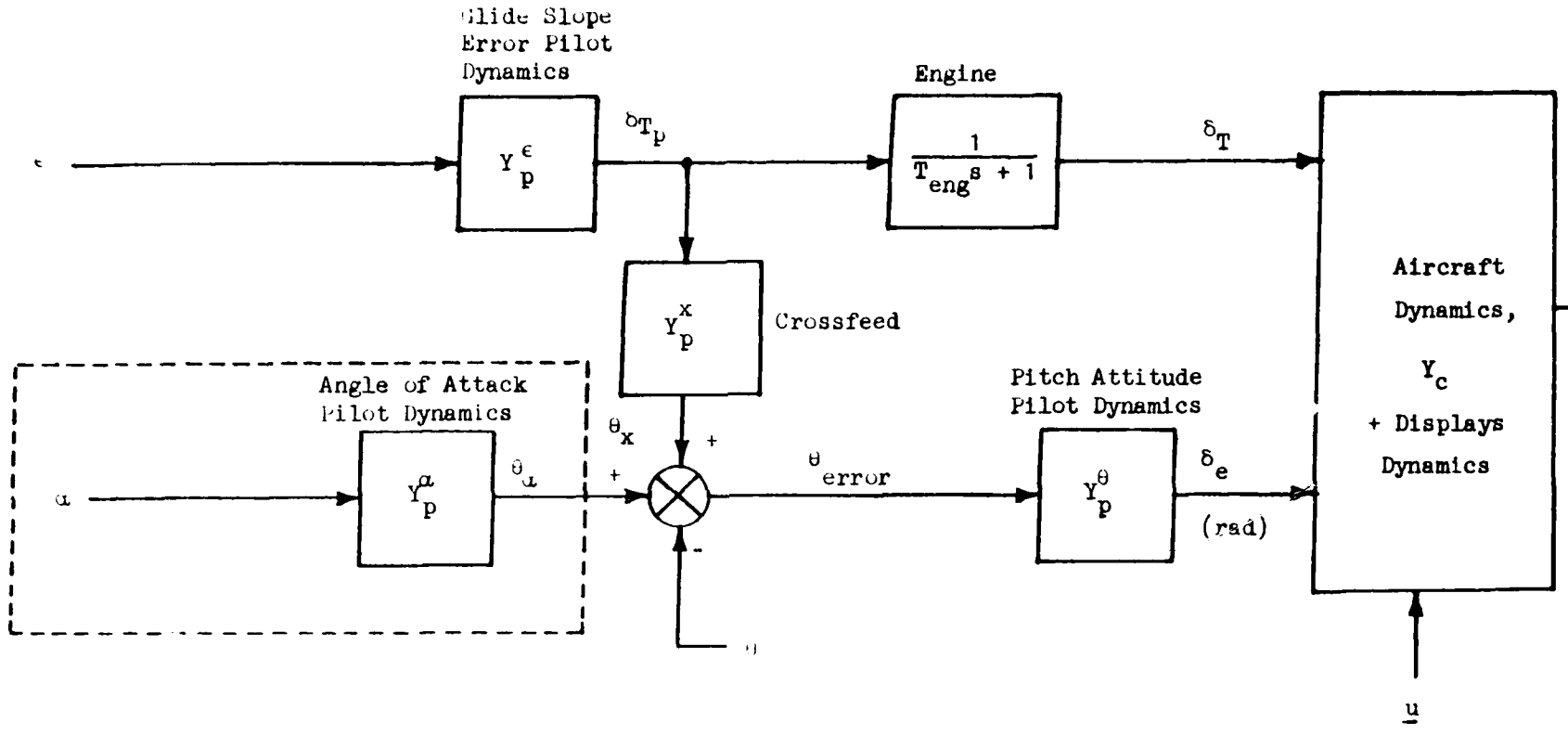

Notes: $\underline{x}$ A vector of the aircraft states (u, w, $\dot{d}$, d, $\dot{\theta}$, θ, etc.)

$\underline{u}$ A vector of external disturbances (u_g, w_g, beam noise, etc.)

Figure 1. Block Diagram of Pilot-Aircraft System

NAVTRAEQUIPCEN 78-C-0060-10

Reference 4 demonstrates that the pursuit-crossfeed piloting technique described above must be used in order to obtain adequate pilot-vehicle performance. Furthermore, once the pilot is established at the reference angle of attack, the crossfeed significantly lessens the need for the $\alpha \rightarrow \delta_e$ loop shown in Fig. 1. The purpose of this report is to show how the control technique depicted in Fig. 1 can be quantified using NIPIP. Specifically, the objective is to quantify the elements of the pilot's control technique, i.e., Y_p^{ε}, Y_p^{x}, and Y_p^{θ}.

NIPIP quantifies the terms Y_p^{ε}, Y_p^{x}, and Y_p^{θ} in terms of frequency-domain describing functions (Ref. 5). The pilot describing functions reflect pilot-behavioral performance and can be used to assess pilot workload. The pilot-alone performance is sometimes a more sensitive measure than the combined pilot-vehicle performance (e.g., rms glide slope deviation, rms airspeed error, etc.) because the pilot adapts to changes in experimental conditions (e.g., vehicle dynamics, display symbology, etc.) in order to maintain the combined-vehicle performance at some acceptable level. For example, the gradual learning of the proper "crossfeed" behavior between the throttle and the elevator inputs can be measured as an index of skill acquisition.

DESCRIPTION OF THE EXPERIMENT

A piloted aircraft simulation was performed on the Visual Technology Research Simulator (VTRS) at the Naval Training Equipment Center (NTEC) at Orlando, Florida. The experiment was conducted by personnel from the Canyon Research Group, Inc., using an experienced Navy pilot. The experimental scenario was as follows:

1. Night approach to an aircraft carrier using a computer-generated image (CGI) display
2. Raw FLOLS display

3. Constant rms turbulence using the sum of sine waves technique described in Table 1. Only the vertical (w_g) and longitudinal (u_g) components were used in this experiment because the lateral component (v_g) was used to simulate beam noise. The rms level for both u_g and w_g was 3.0 fps.

4. No aircraft carrier motion; the beam noise provided a surrogate for the carrier motion artifacts.

The experimental matrix consisted of variations in the following parameters:

1. Constant and variable range from aircraft carrier (i.e., constant range means that the aircraft was not allowed to move closer to the aircraft carrier). Three constant range and one variable range conditions were used:

   a. Variable (normal approach starting from an initial range of 9000 ft)

   b. Constant "long" range (7200 ft)

   c. Constant "medium" range (3600 ft)

   d. Constant "short" range (1800 ft)

2. With and without the simulated beam noise defined in Table 2.

3. "Loose" and "tight" tracking of the glide slope (Student 0 versus Student 2 in Table 3).

The actual experimental matrix is defined in Table 3. The experimental conditions were not randomized.

The T-2C aircraft was used for all of the runs shown in Table 3, and all runs were flown by the same pilot. However, on the "Student 0" runs, the pilot was allowed to fly the (simulated) aircraft as he saw fit. The result was that he did not actively track the glide slope, and admitted

TABLE 1. GUST INPUT SPECTRA FOR T-2C LANDING SIMULATION*

Number of Cycles in 40 sec Run N	Frequency f_i (Hz)	Frequency ω_i (rad/sec)	Gust Shaped Amplitudes for RMS = 1 unit in each Axis: Axial (ft/sec)	Lateral† (ft/sec)	Vertical (ft/sec)	Comments
1	0.025	0.157	A_{u_1} = 0.645			Speed and height modes ω_h
2	0.050	0.314			A_{w_1} = 1.175	
3	0.075	0.471	A_{u_2} = 0.749			
4	0.100	0.628		A_{v_1} = 1.295		Lateral Path Modes ω_ϕ
5	0.125	0.785			A_{w_2} = 0.580	
7	0.175	1.10	A_{u_3} = 0.707			
8	0.200	1.26			A_{w_3} = 0.381	$1/\tau_{\theta_2}$
9	0.225	1.41		A_{v_2} = 0.431		
11	0.275	1.73	A_{u_4} = 0.548			Short Period Mode ω_{sp}
13	0.325	2.04			A_{w_4} = 0.294	
14	0.350	2.20		A_{v_3} = 0.288		
17	0.425	2.67	A_{u_5} = 0.473			Dutch Roll Mode ω_{DR}
19	0.475	2.83			A_{w_5} = 0.226	
23	0.575	3.61		A_{v_4} = 0.234		
			ΣA_i^2 = 2.00	2.0	2.0	

RMS = $(\Sigma A_i^2/2)^{1/2}$ = 1.0 for u_g, v_g, w_g

Each component of turbulence is calculated as follows: $x_g = K_x \Sigma A_i \sin(\omega_i t + \phi_i)$

where $x_g = u_g$, v_g, or w_g;

K_x = scale factor = 3.0 for this simulation(i.e. rms gust level is 3.0 fps);

and ϕ_i are random phase angles that are constant throughout each run but change from run to run.

*Adapted from Ref. 6.

†For this experiment only the lateral components are deleted and are used for beam noise (see Table 2).

TABLE 2. FLOLS BEAM NOISE

Number of Cycles in 40 sec Run	Frequency		Amplitudes
	f_i (Hz)	ω_i (rad/sec)	A_{ε_i} (rad)
4	0.100	0.628	0.003503
9	0.225	1.41	0.003702
14	0.350	2.20	0.001745

$$\Sigma A_{\varepsilon_i}^2 = 2.902E\text{-}5$$

$$\sigma_{\varepsilon_n} = 0.003809 \text{ rad}^*$$

Total beam noise is:

$$\varepsilon_n = K_\varepsilon \Sigma A_{\varepsilon_i} \sin(\omega_i t + \phi_i)$$

Where $K_\varepsilon = 1.0$

Beam noise is injected into FLOLS as follows:

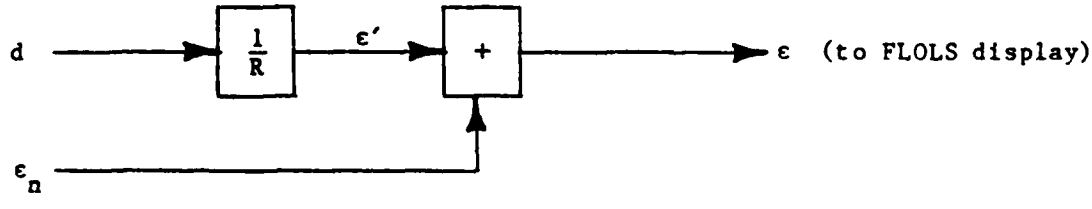

Where

R = range

d = perpendicular distance from nominal glide slope

ε = angular deviation from nominal glide slope

*σ_d = 27 ft at R = 7200 ft

TABLE 3. SUMMARY OF EXPERIMENTAL MATRIX

Configuration No.	Student Code	Range	Beam Noise
	"Loose"		
1a,b,c	0	Variable	OFF
2a,b,c	0	Variable	ON
3a,b	0	Long	OFF
4a,b	0	Long	ON
5a,b	0	Medium	OFF
6a,b	0	Medium	ON
7a,b	0	Short	OFF
8a,b	0	Short	ON
9a,b	0	Variable	OFF
10a,b	0	Variable	ON
	"Tight"		
1a,b,c	2	Variable	OFF
2a,b,c	2	Variable	ON
3a,b	2	Long	OFF
4a,b	2	Long	ON
5a,b	2	Medium	OFF
6a,b	2	Medium	ON
7a,b	2	Short	OFF
8a,b	2	Short	ON
9a,b	2	Variable	OFF
10a,b	2	Variable	ON

that he ignored the beam noise. On the "Student 2" runs, the pilot was told to actively track the glide slope, as would be required to follow low frequency ship motions if they were present.

ANALYSIS

The NIPIP software was used to analyze a select sample of the runs from Table 3. The objectives of the analysis were to discern differences in pilot control strategy due to variation in the following experimental conditions:

1. Constant versus variable range
2. With and without beam noise (surrogate for ship motion)
3. Loose versus tight glide slope tracking

The following runs were selected to meet the objectives defined above:

Loose	Tight
5b.0	5b.2
6a.0	6a.2
9b.0	9b.2
10b.0	10b.2

Time histories for the runs listed above are shown in Figs. 2 through 9. These time histories were used as inputs to the NIPIP software.

The outputs of NIPIP (i.e., $\hat{Y}_p^{\epsilon}$, $\hat{Y}_p^{x}$, and $\hat{Y}_p^{\theta}$) are summarized in Figs. 10 through 15. The figures are arranged as follows: Figs. 10, 11,

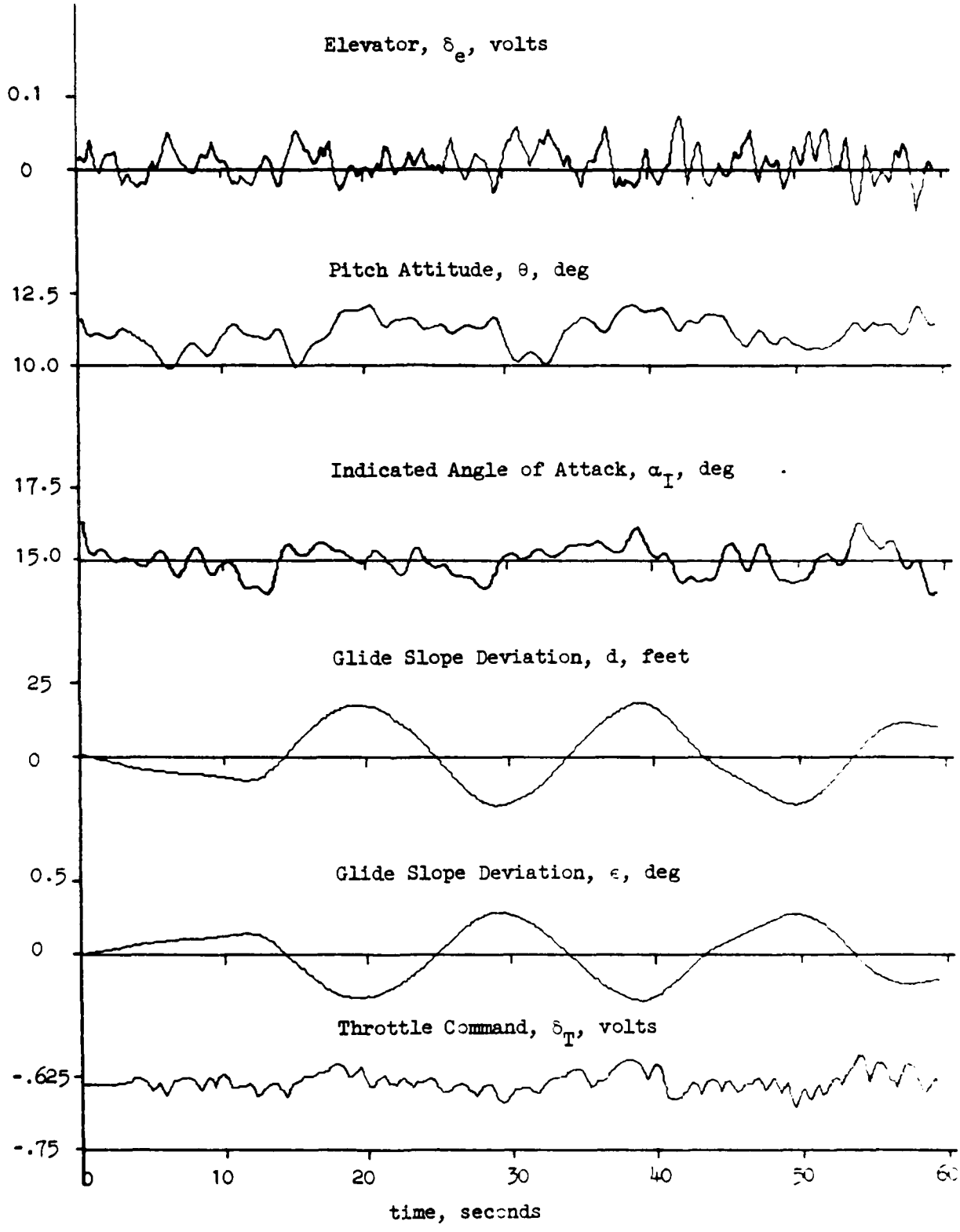

Figure 2. Time History of Configuration No. 5b.0
(Student 0, Constant Range, Beam Noise Off)

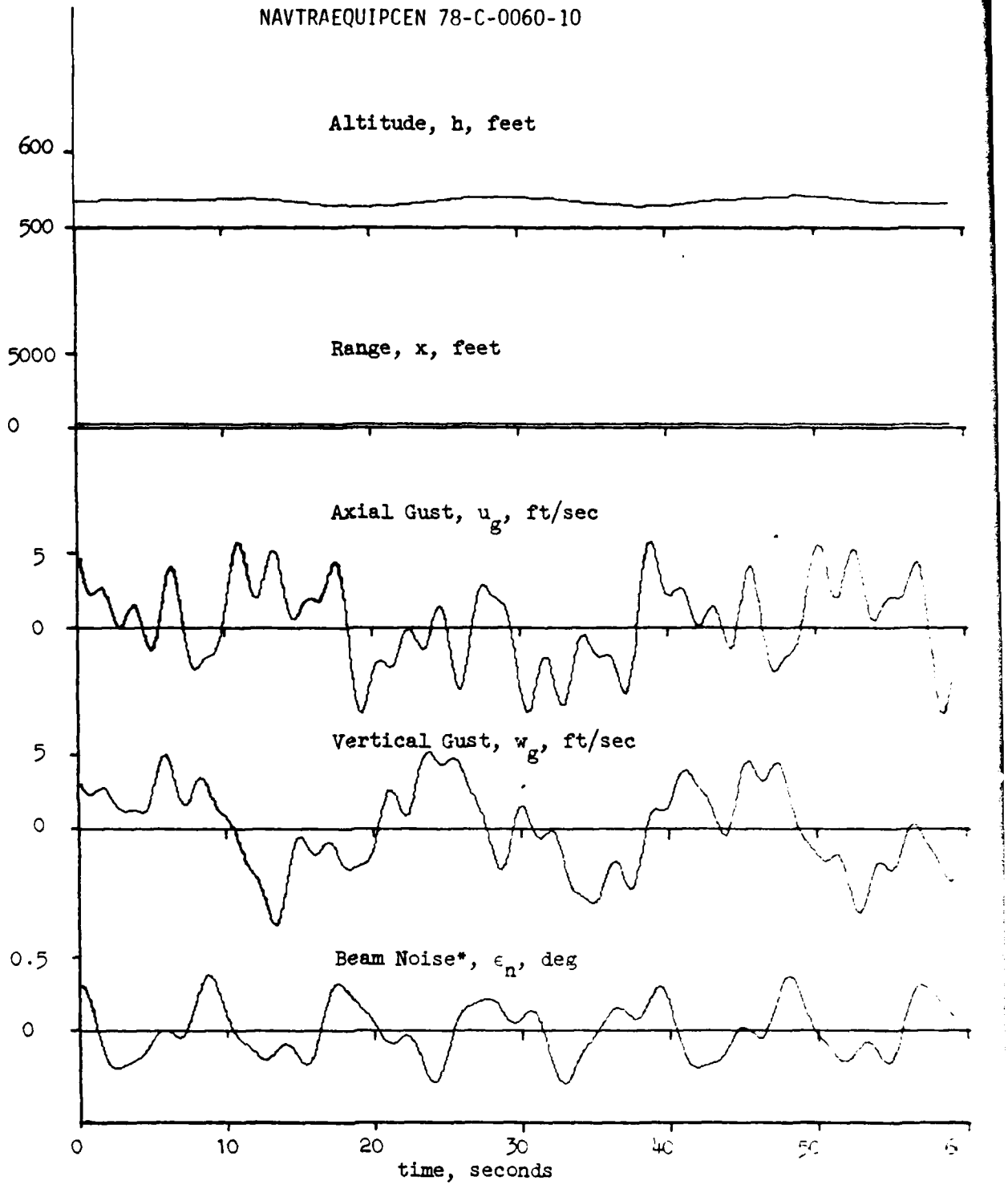

Figure 2 (Concluded)

*ϵ_n not added to ϵ for this run.

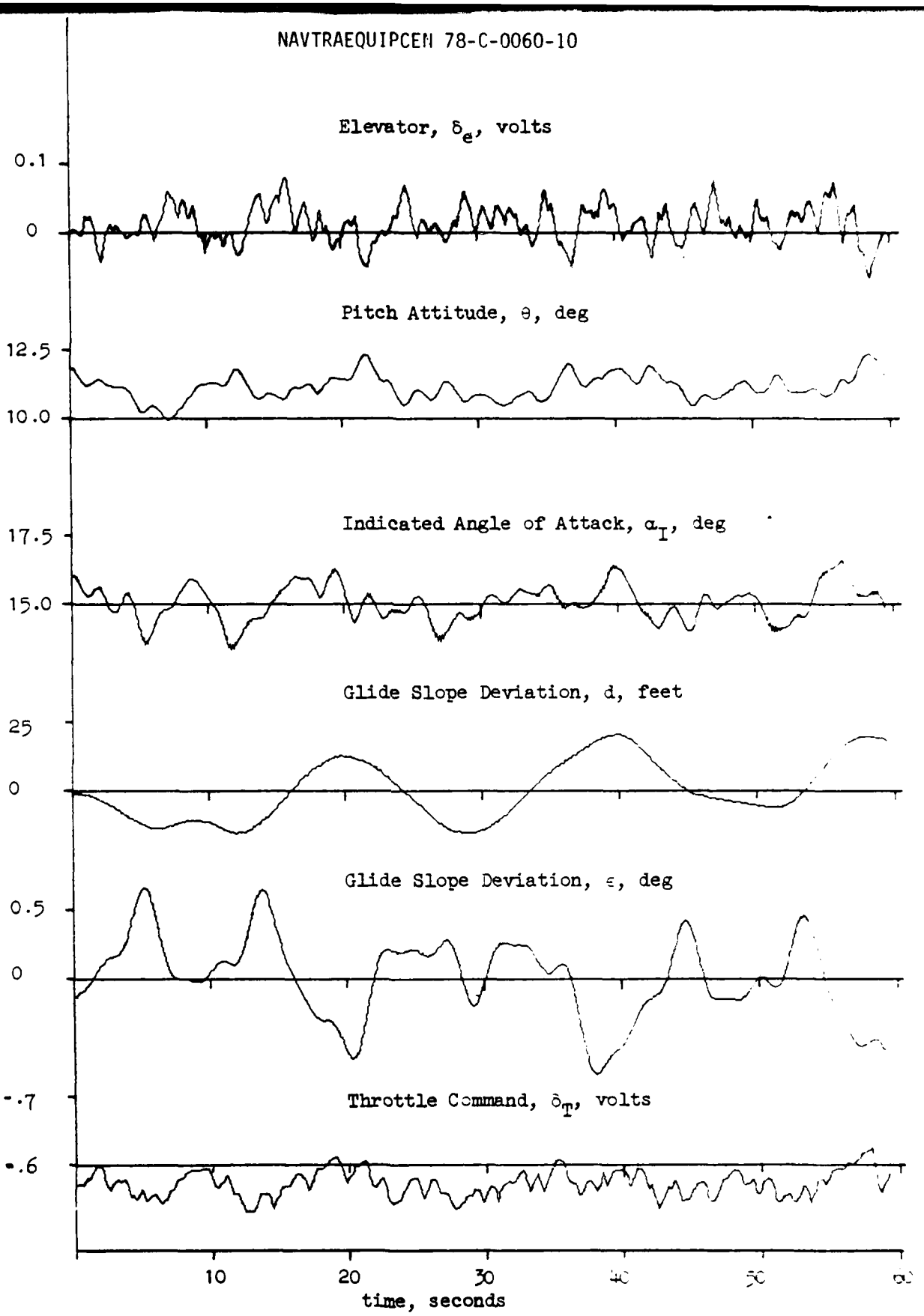

Figure 3. Time History of Configuration No. 6a.0
(Student 0, Constant Range, Beam Noise On)

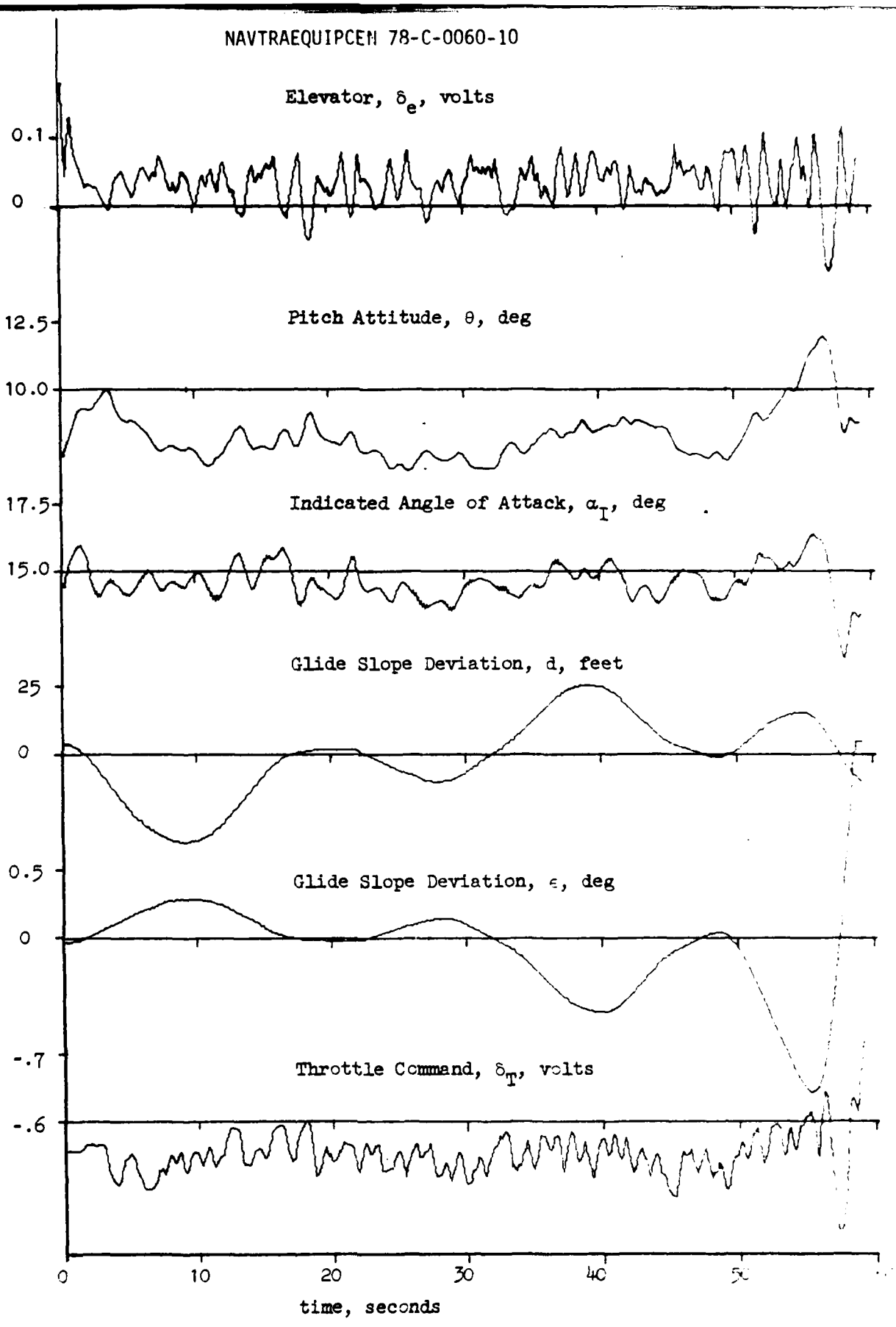

Figure 4. Time History of Configuration No. 9b.0
(Student 0, Variable Range, Beam Noise Off)

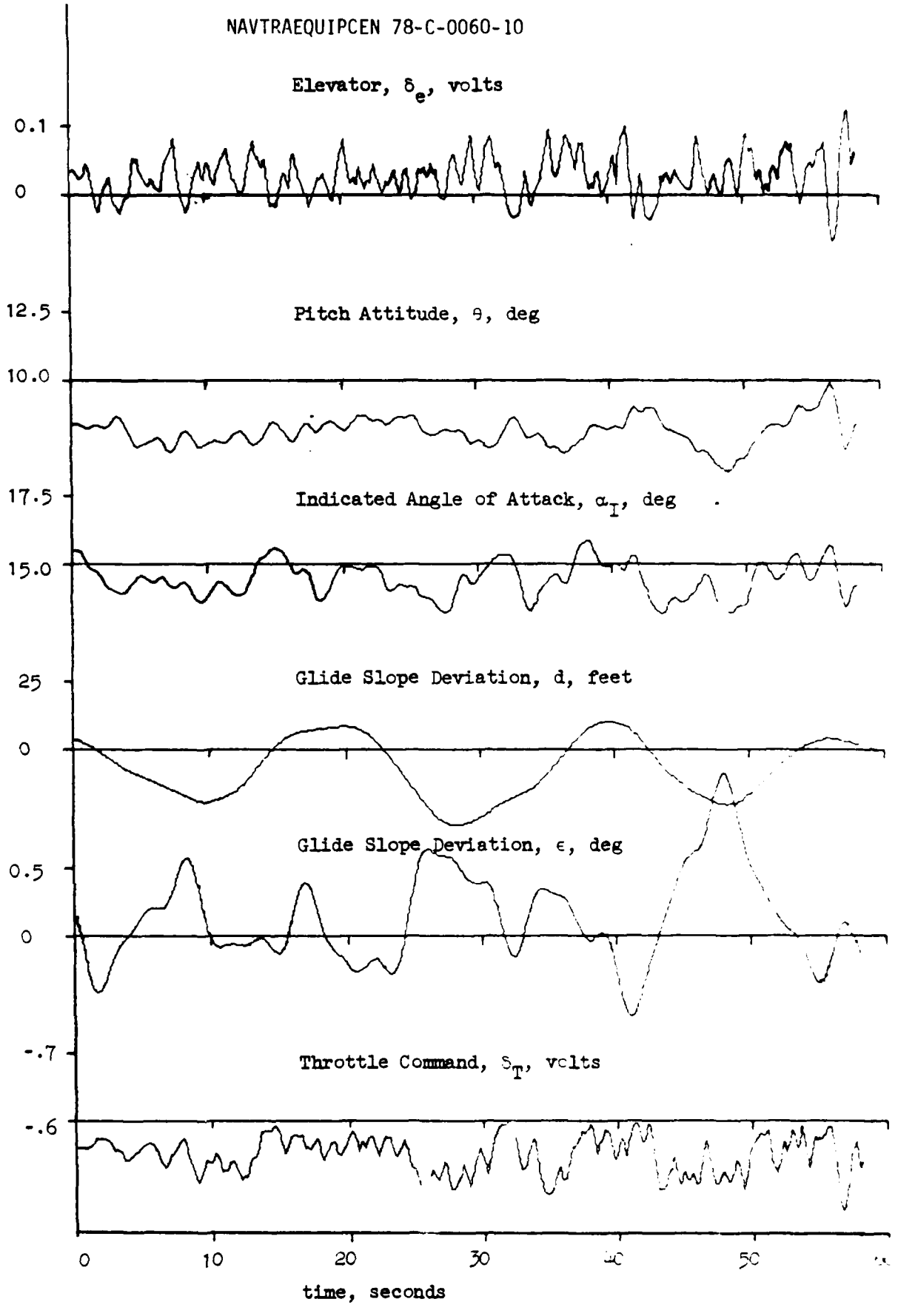

Figure 5. Time History of Configuration No. 10b.0 (Student 0, Variable Range, Beam Noise On)

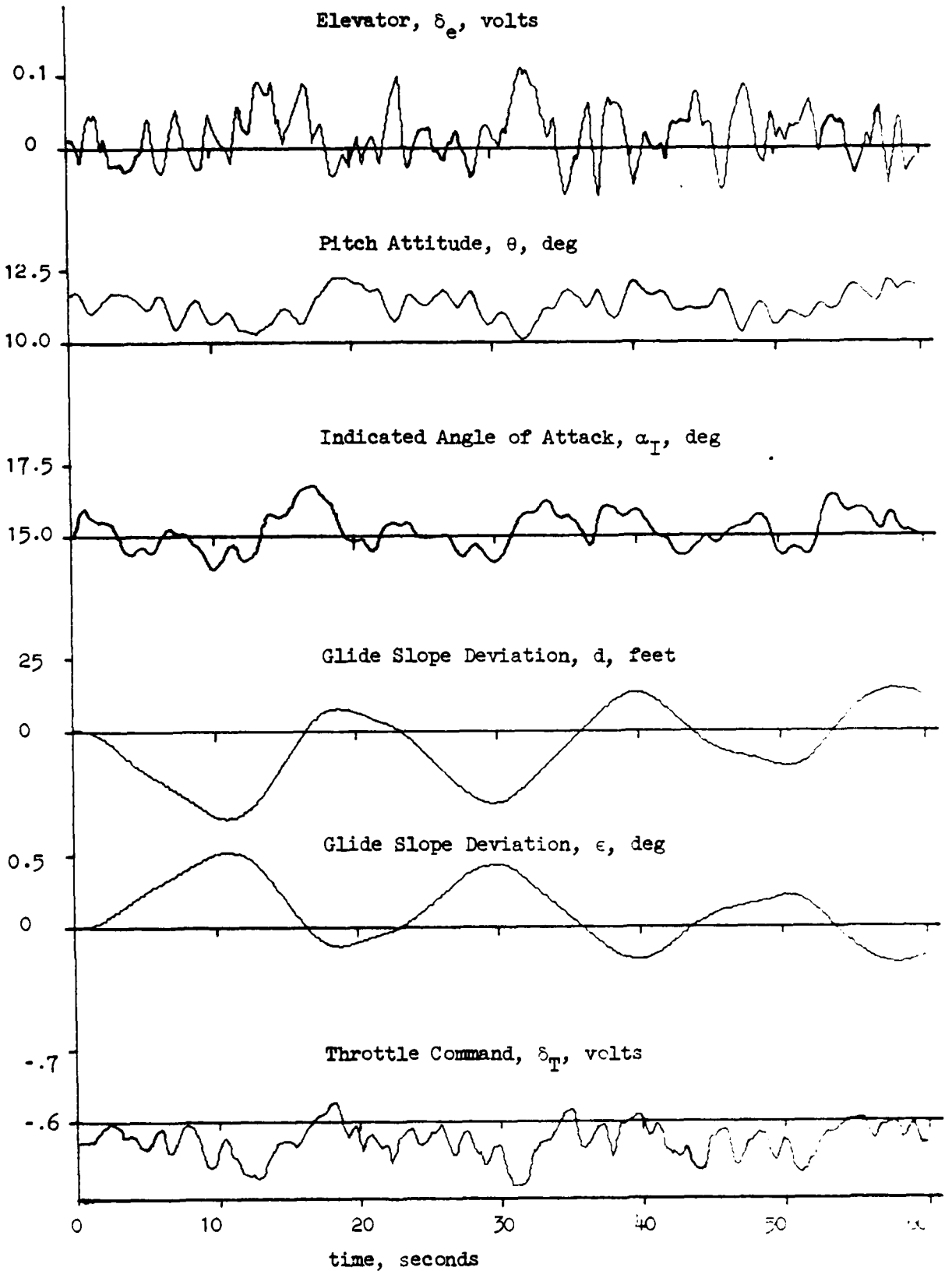

Figure 6. Time History of Configuration No. 5b.2
(Student 2, Constant Range, Beam Noise Off)

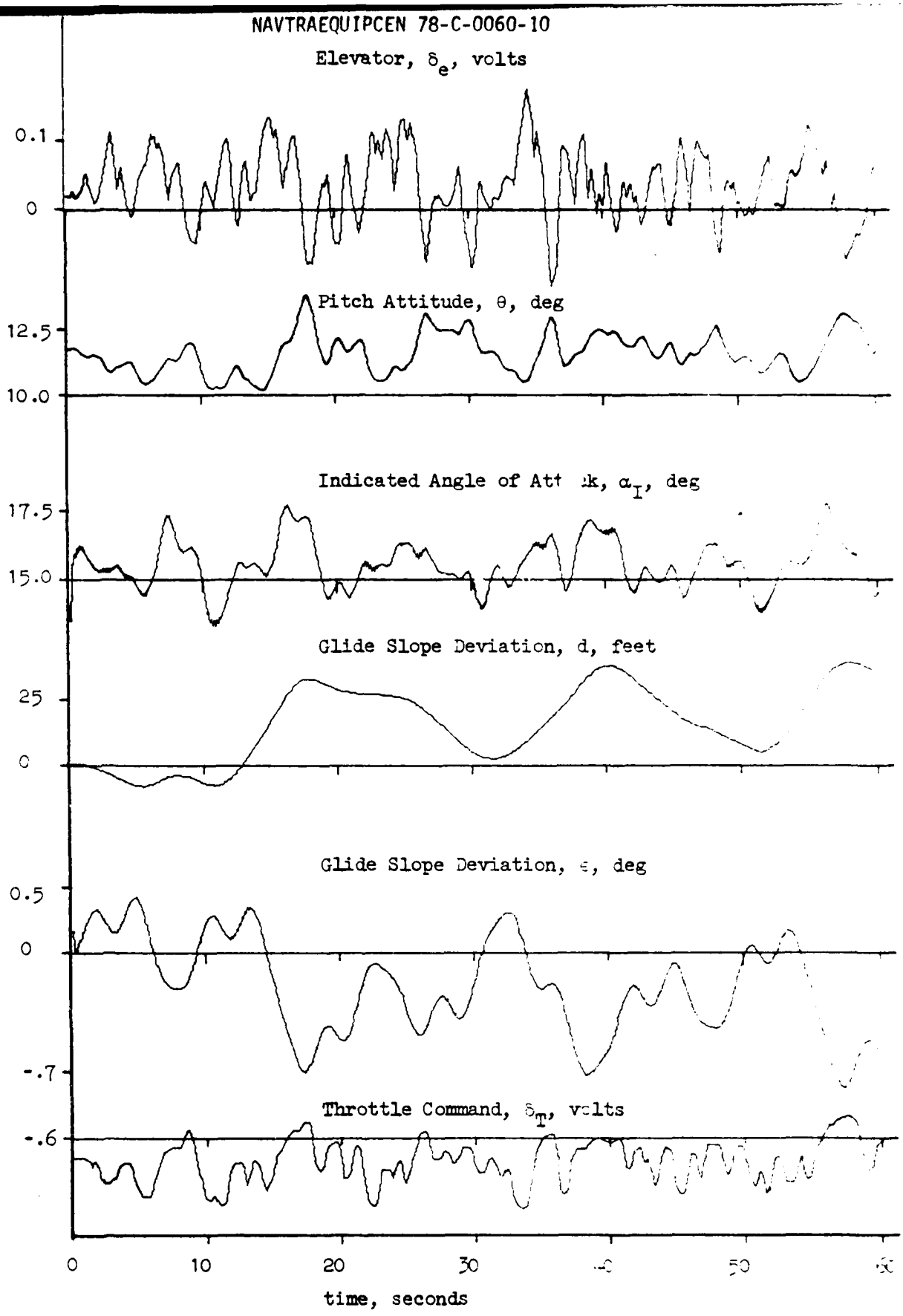

Figure 7. Time History of Configuration No. 6a.2
(Student 2, Constant Range, Beam Noise On)

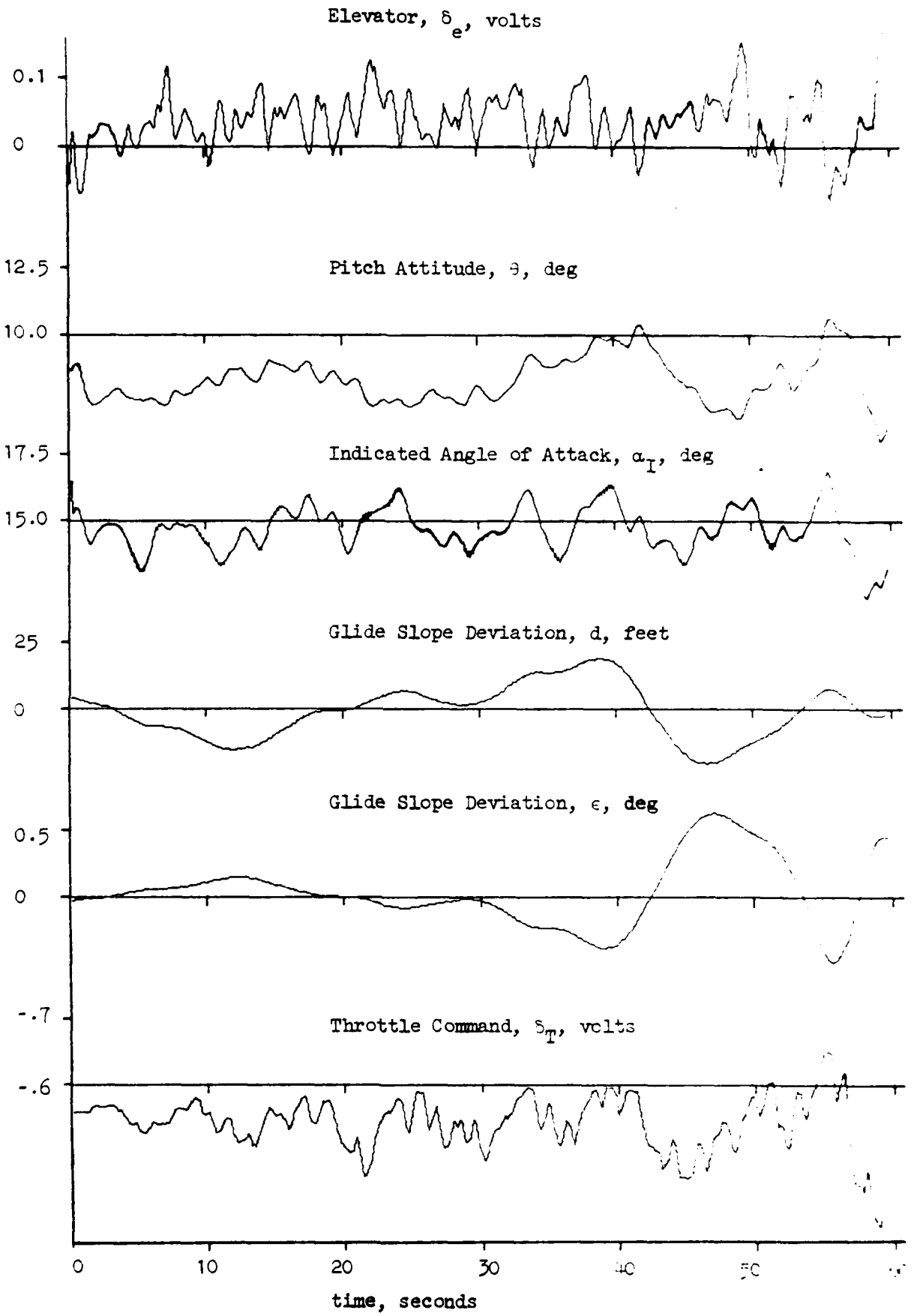

Figure 8. Time History of Configuration No. 9b.2
(Student 2, Variable Range, Beam Noise Off)

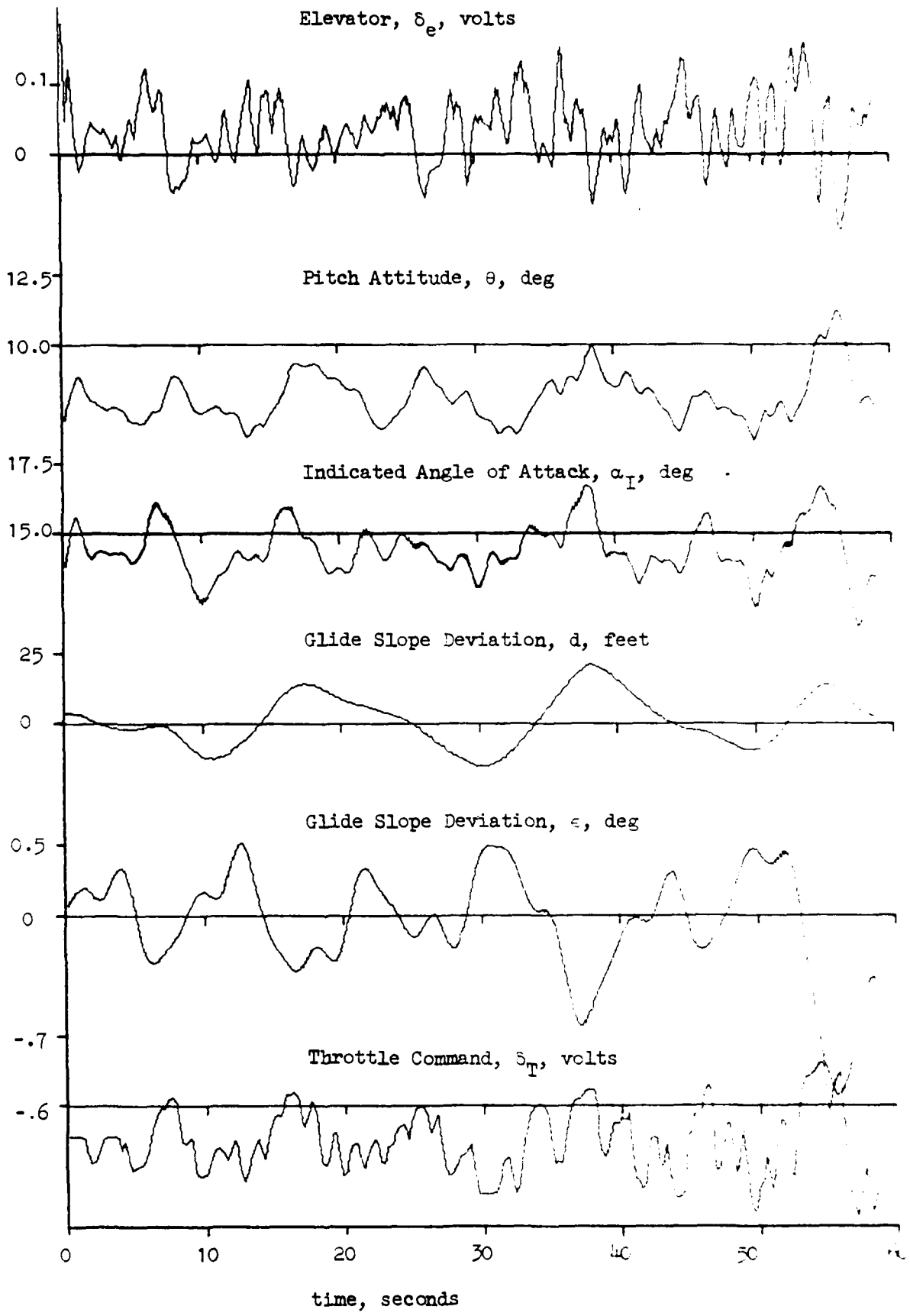

Figure 9. Time History of Configuration No. 10b.2
(Student 2, Variable Range, Beam Noise On)

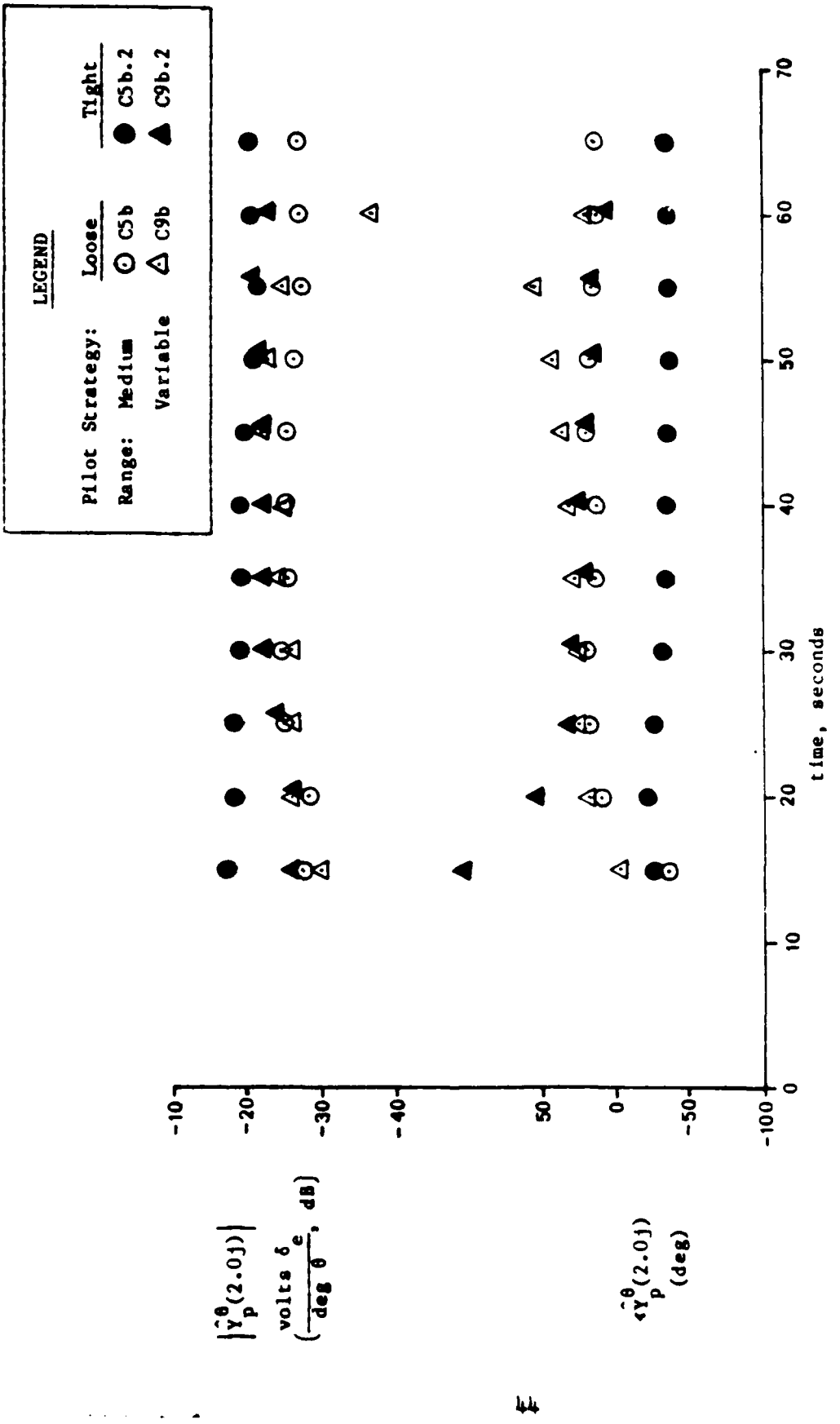

Figure 1 . Time History of Pitch Loop Describing Function, $\hat{Y}^{\theta}_{p}(j\omega)$, No Beam Noise Configurations

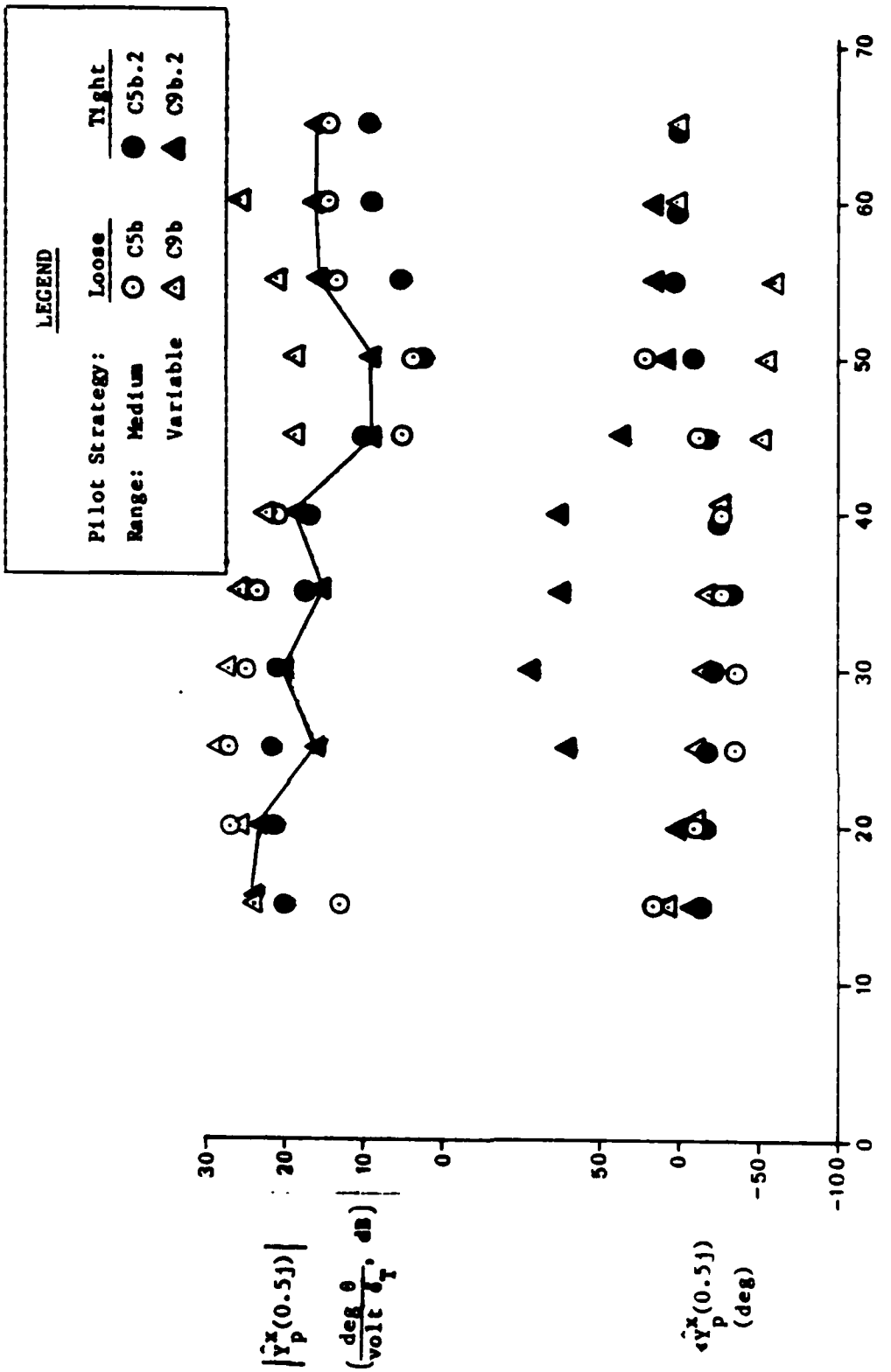

Figure 11. Time History of Crossfeed Describing Function, $\hat{Y}^{x}_{p}(j\omega)$, No Beam Noise Configurations

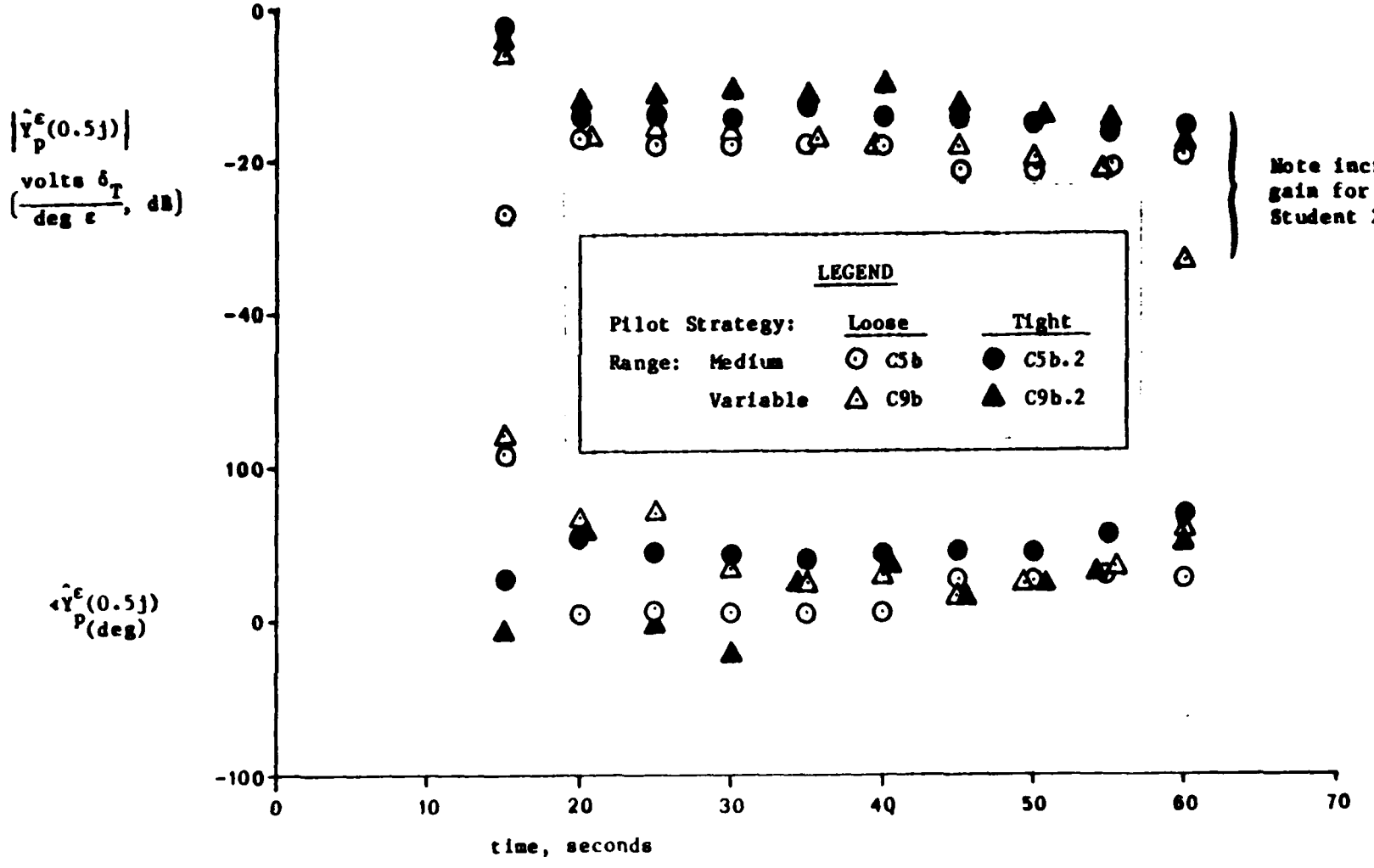

NAVTRAEQUIPCEN 78-C-0060-10

Figure 12. Time History of Glide Slope Loop Describing Function, $\hat{Y}_p^{\epsilon}(j\omega)$, No Beam Noise Configurations

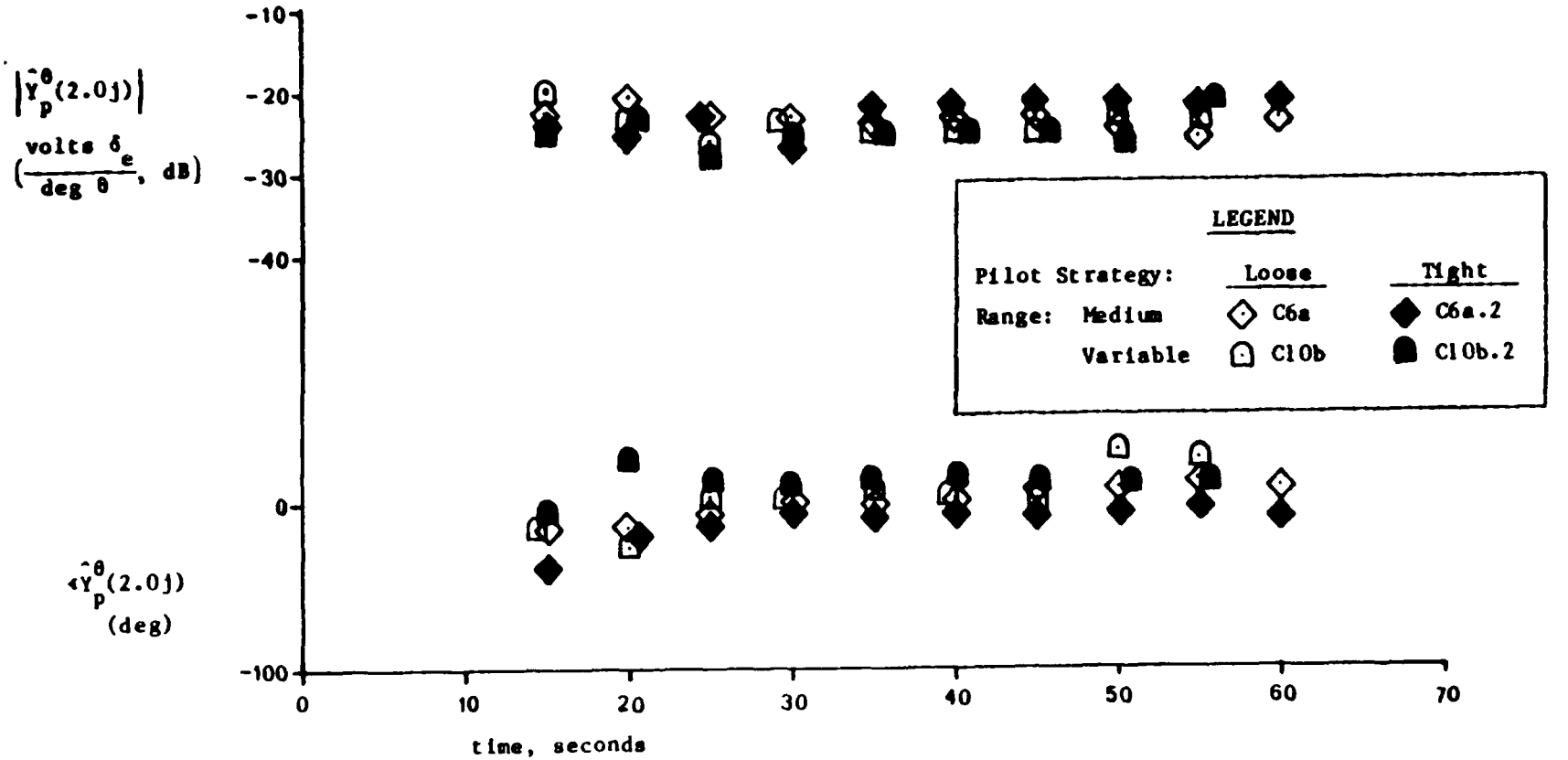

Figure 15. Time History of Pitch Loop Describing Function, $\hat{Y}_p^{\theta}(j\omega)$, With Beam Noise Configurations

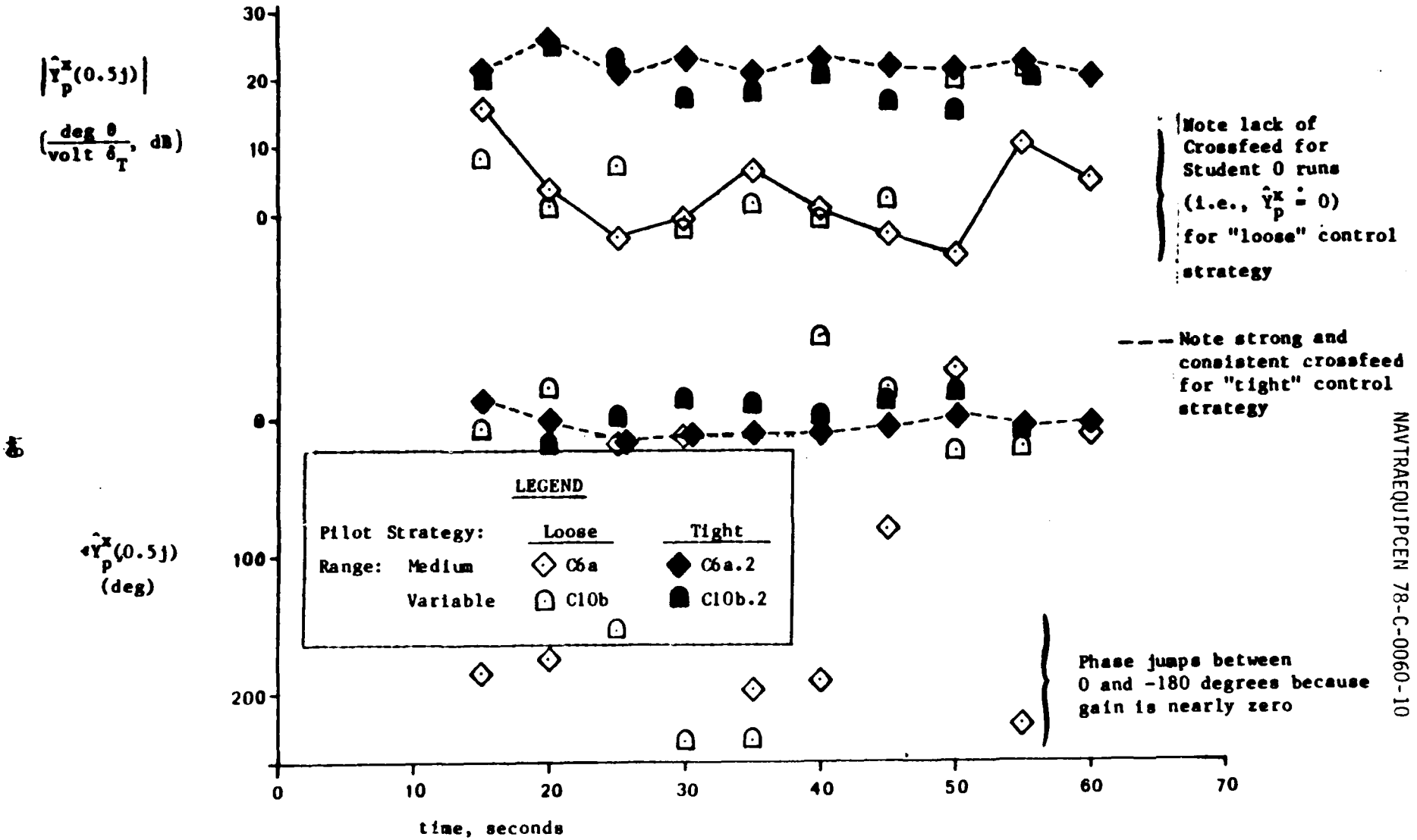

Figure 14. Time History of Crossfeed Describing Function, $\hat{Y}_p^x(j\omega)$, With Beam Noise Configurations

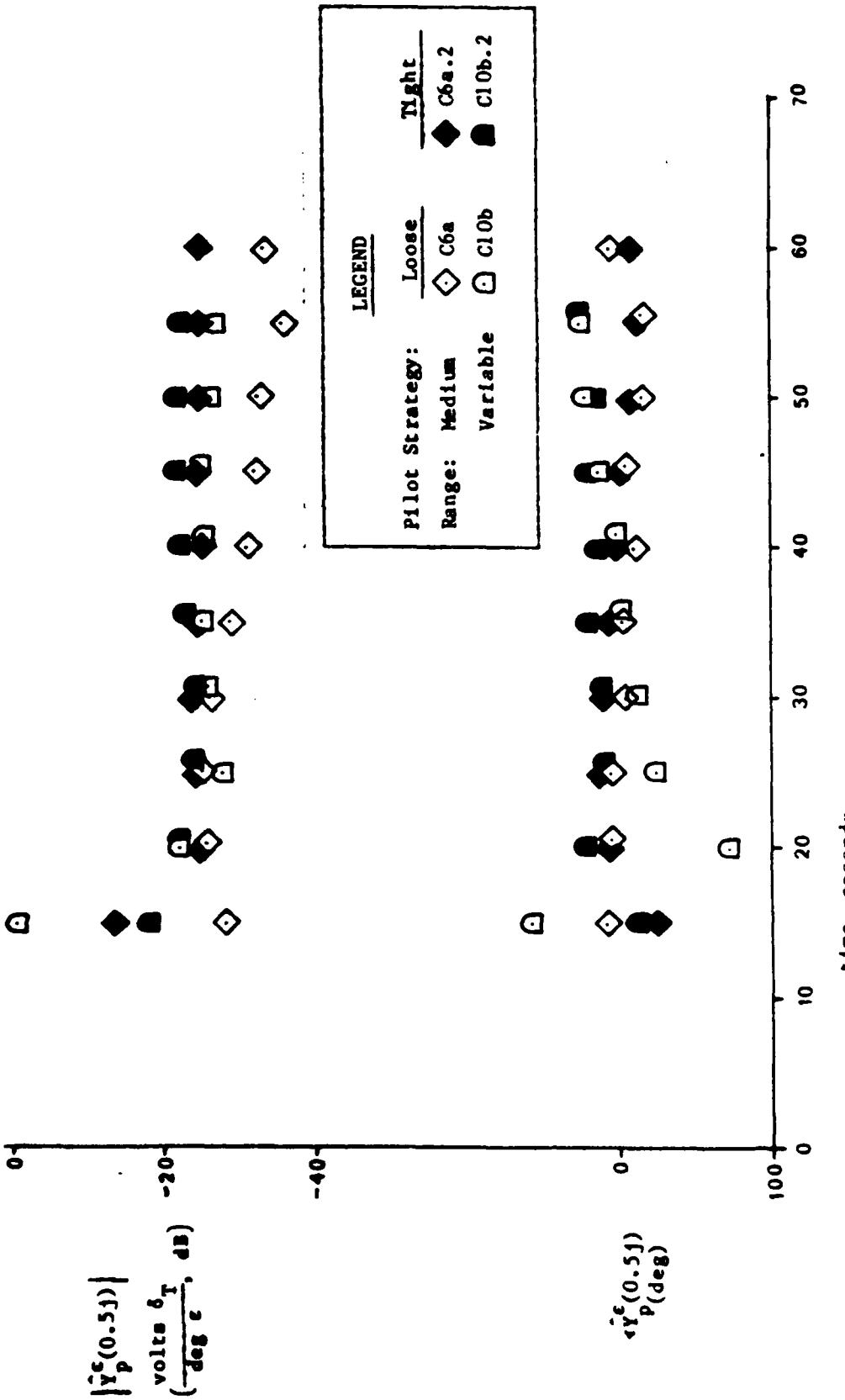

Figure 1... Time History of Glide Slope Loop Describing Function, $\hat{Y}^{\epsilon}_{p}(j\omega)$, With Beam Noise Configurations

and 12 are $\hat{Y}_p^{\theta}$, $\hat{Y}_p^{x}$, and $\hat{Y}_p^{\varepsilon}$, respectively, for all of the no-beam-noise runs (5b.0, 9b.0, 5b.2 and 9b.2); Figs. 13, 14, and 15 are the equivalent describing functions for the runs with beam noise (6a.0, 10b.0, 6a.2, 10b.2).

The time history of each describing function is presented as an amplitude ratio (dB) and phase (deg) at a single frequency, where

$$\left|Y_p(j\omega)\right|_{dB} = 20 \log_{10} \left|Y_p(j\omega)\right|$$

Thus the amplitude plots of $Y_p(j\omega)$ are logarithmic scales (e.g., a 20 dB change in $\left|Y_p(j\omega)\right|$ is a factor of 10, a 6 dB change is a factor of 2). The phase plots indicate the relative amounts of lead or lag between the control and the variable to be controlled.

While the describing function at each frequency exists at each computed time, its value near the crossover-frequency region of each loop is of key importance. Therefore we have chosen to illustrate Y_p at 2.0 volts/sec (about 1/3 Hz) for inner loops (θ) and 0.5 volts/sec (about 0.1 Hz) for outer loops (x and ε).

The legend used to plot the data in Figs. 10 through 15 is as follows:

1. Open symbols were "loose" tracking ("Student 0," pilot not following beam noise)
2. Closed symbols are "tight" tracking ("Student 2," pilot told to follow beam noise)
3. The symbols used were:

   Medium range, $\varepsilon_n = 0$, Configuration 5

   Medium range, $\varepsilon_n \neq 0$, Configuration 6

Variable range, $\epsilon_n = 0$, Configuration 9

Variable range, $\epsilon_n \neq 0$, Configuration 10

A sliding time window of 30 seconds was used for all of the data presented in Figs. 10 through 15. Also, the first 10 seconds of each run was ignored; and NIPIP waits 5 seconds before outputting the estimates of $Y_p(j\omega)$. Thus there is no output from NIPIP until t = 15 seconds in all of the figures.

Conclusions and observations based on the time histories shown in Figs. 10 through 15 are presented in the next subsection.

CONCLUSIONS AND OBSERVATIONS

The following conclusions and observations are based on the somewhat small data base presented in the previous section. In order to substantiate these findings, we recommend that a larger amount of data be analzyed. It is not the purpose of this report to make broad statements on pilot control techniques; rather, the main purpose of this report is to demonstrate the kinds of conclusions that can be made by using the NIPIP software.

Pitch Loop

There were no consistent changes in the pitch attitude describing function, $Y_p^{\theta}(j\omega)$, with changes in experimental conditions. Except for Configuration 5b.2 in Fig. 10, the pilot tended to use a slight amount of lead ($\angle Y_p^{\theta}(2.0j) \approx 0$ to +25 deg), and a gain between -20 dB and -25 dB. This lack of trends in the $\hat{Y}_p^{\theta}(j\omega)$ data indicates that the inner-loop closure on $\theta \rightarrow \delta_e$ is relatively independent of simulated beam noise or tightness of the glide slope loop. This makes sense because the pilot

must always closely stabilize the pitch attitude of the aircraft against disturbances by using the elevator, and the tightness of this loop is set mainly by aircraft constraints (Ref. 5).

Crossfeed

There were some very interesting and consistent trends in the crossfeed $\hat{Y}_p^x(j\omega)$. For the runs with beam noise (Fig. 13) the pilot used a very high crossfeed gain for the "Student 2" runs, but virtually no crossfeed for the "Student 0" runs, where beam noise was ignored. Also note that the gain was practically the same for both the constant and the variable range runs for "Student 2" but not for "Student 0." This is consistent with the experimental conditions because, for the "Student 2" runs, the pilot was told to actively track the glide slope; but, for the "Student 0" runs, the pilot admitted that he was ignoring the glide slope disturbances. More about this result will be stated shortly.

There was much more variability and a lack of consistent trends in $\hat{Y}_p^x(j\omega)$ data for the no beam noise runs (Fig. 11). These results indicate a lack of consistent piloting technique when there is an insufficient disturbance in glide slope deviation. This result has some important implications with respect to pilot training. First, the pilot-aircraft system must be disturbed from the nominal glide slope in order for the pilot to learn (and hence to demonstrate) the proper control techniques. The simulated beam noise used in this experiment provided the required disturbance, but the pilot thought it was unrealistic. Indeed, the pilot tried to ignore the beam noise during the initial set of runs ("Student 0"). A more realistic glide slope disturbance could be easily provided by using wind shears starting during different portions of the final approach. This would not only force the pilot to use the proper control technique but would also acquaint him with the limitations of the aircraft (e.g., when he should wave-off versus reacquiring the glide slope and continuing to a landing).

Glide Slope

There were also some interesting trends in the flight path control describing function, $\hat{Y}_p^{\varepsilon}(j\omega)$. The "Student 2" gains, $\left|\hat{Y}_p^{\varepsilon}(j\omega)\right|$, were consistently higher than the "Student 0" gains (shaded versus open symbols in Figs. 12 and 15), and the variability in the data with beam noise (Fig. 15) was generally lower than in the data without beam noise (Fig. 12), especially in the phase angles, $\angle \hat{Y}_p^{\varepsilon}(j\omega)$. The higher gains indicate higher pilot workload, and the low variability in the phase angles indicate a more consistent pilot control strategy. These trends are similar to the Y_p^x data discussed above and are consistent with the experimental conditions.

SUMMARY

The NIPIP software was successfully used to analyze selected runs from an aircraft simulation of the T-2C on final approach to an aircraft carrier. NIPIP quantifies the pilot's control strategy in terms of frequency-domain describing functions. The parameters of these describing functions are gains and phase angles, which can be used to infer pilot workload and performance. For example, a high gain indicates tight closed-loop control (high bandwidth) but also demands high pilot workload. A positive phase angle indicates that the pilot is generating lead in his control technique —— a process which also increases workload. A negative phase angle indicates a lag smoothing control technique.

The NIPIP results presented herein were consistent with the various experimental conditions. The most interesting results were the changes in the pilot's describing functions with simulated glide slope disturbances (injected beam noise) and the "tight" versus "loose" tracking runs. For the "loose" tracking runs, there was a very low glide slope gain and virtually no crossfeed gain. For the "tight" tracking runs, the pilot exhibited high glide slope and crossfeed gains with relatively low

variability in the data, especially for the runs with beam noise. The implication is that adequate glide slope disturbances must be present in order for the pilot to demonstrate his ability to control the aircraft properly, as discussed above.

The main objective of this experiment was fulfilled in that NIPIP was able to discern differences in pilot control strategy under simulated flight conditions. However, it is recommended that further testing be done using a number of pilots (both skilled and trainees) under controlled experimental conditions.

REFERENCES FOR SECTION IV

1. Jewell, Wayne F., and Ted M. Schulman, A Pilot Control Strategy Identification Technique for Use in Multiloop Control Tasks, Systems Technology, Inc., Technical Report No. 1153-2, August 1980.

2. Jewell, Wayne F., Application of the Non-Intrusive Pilot Identification Program to a Multiloop Control Task, Systems Technology, Inc., Working Paper No. 2122-5, December 1980.

3. Jewell, Wayne F., Identification of Multiloop Pilot Describing Functions Obtained from Simulated Approaches to an Aircraft Carrier, Systems Technology, Inc., Paper No. 289, Presented at the 17th Annual Conference on Manual Control, UCLA, June 16-19, 1981.

4. Clement, Warren F., and Robert K. Heffley, An Example of a Concept for Establishing Flight Training Media Requirements, Systems Technology, Inc., Technical Report No. 2108-1, May 1980.

5. McRuer, Duane, Irving Ashkenas, and Dunstan Graham, Aircraft Dynamics and Automatic Control, Princeton University Press, Princeton, New Jersey, 1973.

6. Jex, Henry R., and Raymond E. Magdaleno, Quasirandom Gust Inputs for the T2C Simulation at NTEC, Systems Technology, Inc., Working Paper No. 2122-1, 30 June 1980. (Section II, herein.)

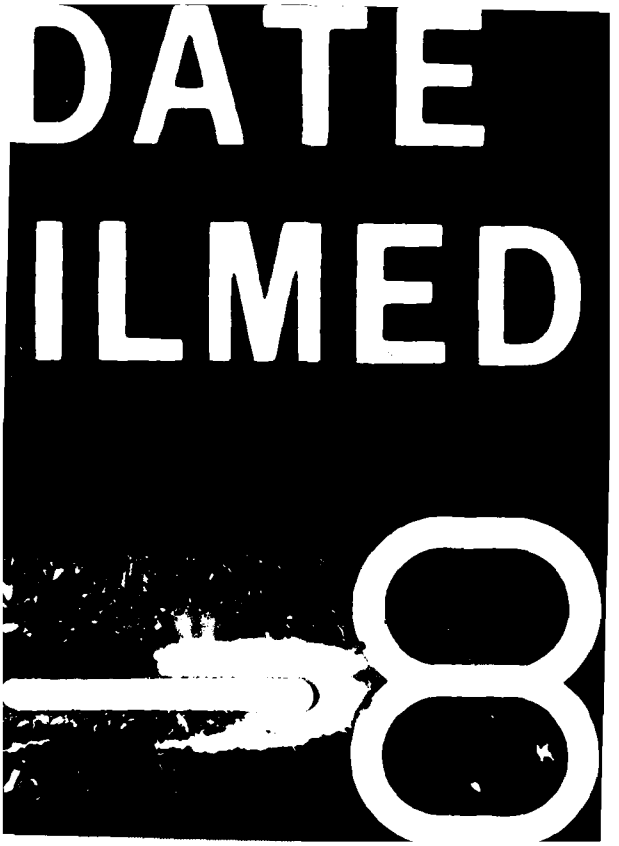
DATE
ILMED
8